

MULTILEVEL ADAPTIVE SPARSE LEJA APPROXIMATIONS FOR
BAYESIAN INVERSE PROBLEMS*

I.-G. FARCAȘ†, J. LATZ‡, E. ULLMANN‡, T. NECKEL†, AND H.-J. BUNGARTZ†

Abstract. Deterministic interpolation and quadrature methods are often unsuitable to address Bayesian inverse problems depending on computationally expensive forward mathematical models. While interpolation may give precise posterior approximations, deterministic quadrature is usually unable to efficiently investigate an informative and thus concentrated likelihood. This leads to a large number of required expensive evaluations of the mathematical model. To overcome these challenges, we formulate and test a multilevel adaptive sparse Leja algorithm. At each level, adaptive sparse grid interpolation and quadrature are used to approximate the posterior and perform all quadrature operations, respectively. Specifically, our algorithm uses coarse discretizations of the underlying mathematical model to investigate the parameter space and to identify areas of high posterior probability. Adaptive sparse grid algorithms are then used to place points in these areas and ignore other areas of small posterior probability. The points are weighted Leja points. As the model discretization is coarse, the construction of the sparse grid is computationally efficient. On this sparse grid, the posterior measure can be approximated accurately with few expensive, fine model discretizations. The efficiency of the algorithm can be enhanced further by exploiting more than two discretization levels. We apply the proposed multilevel adaptive sparse Leja algorithm in numerical experiments involving elliptic inverse problems in two- and three-dimensional space, in which we compare it with Markov chain Monte Carlo sampling and a standard multilevel approximation.

Key words. Bayesian inference, multilevel method, adaptive sparse grids, partial differential equation

AMS subject classifications. 35R30, 62F15, 65C60, 65D30, 65N30, 68T05

DOI. 10.1137/19M1260293

1. Introduction. Mathematical models in science and engineering often require input parameters which cannot be observed directly, yet these parameters are required for predictions based on the model. A standard procedure is to estimate the inputs from indirect observations, which is known as an *inverse problem*. In contrast, the corresponding *forward problem* maps from the parameter to the observation space.

In many applications, for instance, the geosciences or medical sciences, the observations are noisy and their number is insufficient to identify a unique associated parameter value. The Bayesian approach to inverse problems [24, 44, 47] provides a consistent mechanism to combine noisy or incomplete data with prior knowledge and to quantify the uncertainty in the parameter estimate. The prior knowledge is incorporated into a probability distribution over the parameter space; this is termed *prior (measure)* μ_0 . The Bayesian solution to the inverse problem is then the *posterior (measure)* μ^y arising from conditioning the prior μ_0 on the observations y . Unfortunately, the posterior is often intractable in the sense that it does not admit closed form analytic expressions. Hence approximations have to be used in practice.

*Submitted to the journal's Methods and Algorithms for Scientific Computing section May 6, 2019; accepted for publication (in revised form) December 2, 2019; published electronically February 19, 2020.

<https://doi.org/10.1137/19M1260293>

Funding: This work was supported by the German Research Foundation (DFG) through the TUM International Graduate School of Science and Engineering (IGSSE) within Project 10.02 BAYES and by the EPSRC under grant EP/R014604/1.

†Department of Informatics, Technical University of Munich, 85748 Garching, Germany (farcasi@in.tum.de, neckel@in.tum.de, bungartz@in.tum.de).

‡Department of Mathematics, Technical University of Munich, 85748 Garching, Germany (jonas.latz@ma.tum.de, elisabeth.ullmann@ma.tum.de).

Sampling-based posterior approximations such as Markov chain Monte Carlo (MCMC) [1] or sequential Monte Carlo [7] do not rely on the smoothness of the parameter-to-observation map and can be conducted in high-dimensional parameter spaces. The drawback is that without exploiting smoothness or low-dimensional structure in the parameter space often a prohibitive number of samples are required to obtain the desired accuracy. Since each sample entails the evaluation of the forward map, the total cost of the Bayesian inversion becomes prohibitive if the forward model is specified by a partial differential equation (PDE) and is thus computationally expensive. In recent years, many works have suggested computationally feasible yet accurate approximations of the posterior. In this work we focus on *sampling-free* approximations for computationally expensive problems for parameter spaces of small to moderate dimension. We assume that the prior and posterior have a probability density function with respect to (w.r.t.) the Lebesgue measure and approximate the posterior density using sparse grid interpolation and sparse grid quadrature.

Sampling-free approaches often involve *surrogates* for the forward response operator to decrease the computational cost. Typical surrogates are based on generalized polynomial chaos [11, 29, 33, 51], sparse grids [3, 5, 31, 39, 40, 41], Gaussian process regression [25, 45], model reduction [15, 27, 30], and combinations, e.g., sparse grids and reduced bases [3, 4]. To obtain an accurate (and convergent) approximation, these surrogates require certain types of smoothness of the response surface or likelihood function w.r.t. the input parameters. The smoothness assumptions can be weakened by using piecewise polynomial approximations together with Voronoi tessellations of the parameter space [34]. Of course, surrogates can also be used to accelerate sampling-based approximations such as MCMC; see, e.g., [29, 36]. We remark that quasi-Monte Carlo [8, 38] is in principle a sampling-free method which does not rely on surrogates; however, it requires again a smooth approximand and is often used together with randomization.

Theoretical analysis shows that if the surrogate converges to the forward model at a specific rate w.r.t. the prior weighted L^2 -norm, then the approximate posterior converges to the exact posterior with at least the same rate [33, 44]. This result has been improved recently in [50], where it was shown that the convergence rate of the posterior approximation is at least twice as large as the convergence rate of the surrogate, for general priors. However, constructing an accurate surrogate over the entire support of the prior might not be feasible and is in fact often unnecessary. Indeed, in inference problems where the data is informative, the posterior differs significantly from the prior and is supported only in a small part of the prior support. This suggests adapting and localizing the surrogate construction to the support of the posterior. We adopt this approach in our work and construct multilevel, adaptive surrogates with localized support using adaptive sparse grid approximations.

The idea of posterior-focused surrogates is not new; it has, however, received little attention to date in the literature. Li and Marzouk [29] borrow ideas from statistics and construct an efficient polynomial chaos surrogate associated with a density that minimizes the cross entropy between the posterior and a family of multivariate normal distributions. Jiang and Ou [23] suggest a two-stage surrogate based on generalized multiscale finite elements (FEs) and least-squares stochastic collocation. Yan and Zhou [51] propose a multifidelity polynomial chaos surrogate which combines a large number of inexpensive low-fidelity model evaluations with a small number of expensive high-fidelity model evaluations, following the idea of multifidelity approximations [37]. Moreover, Chen, Villa, and Ghattas [5] proposed using a Laplace approximation of the posterior at the maximum a posteriori point to efficiently perform adaptive sparse grid quadrature in Bayesian inverse problems with Gaussian prior.

One challenge of posterior-focused surrogates is the need to handle arbitrary densities which can deviate significantly from the prior which is usually a classical density such as uniform or Gaussian. We address this by constructing adaptive sparse grid approximations based on *weighted (L)-Leja sequences* (see, e.g., [12, 22, 35]). Note that sparse grid approximations with Leja points have been devised for forward uncertainty propagation in [13, 14, 16, 35]. In [13] the adaptive construction of the points is guided by sensitivity scores, and the strategy is applied in plasma microturbulence analysis. In [16] the Leja points are constructed with the help of an adjoint-based error indicator. The use of Leja points to approximate posterior densities is a novel contribution to the literature. Leja points offer further computational advantages since they are *nested* and thus allow one to reuse (expensive) model evaluations.

To address the computational challenges of high-dimensional Bayesian inversion, we use multilevel approximations. At each level, *dimension-adaptive* sparse grids [6, 17, 35] are employed, either in standard form or using directional variances to better exploit anisotropies in the parameter space. In particular, at the first level, our algorithm uses a coarse discretization of the given model to investigate the parameter space and to identify areas of high posterior probability. Adaptive algorithms are then used to place weighted (L)-Leja points in these areas and ignore other areas of small posterior probability. Starting with the second level, we sequentially update the auxiliary reference density such that the previous sparse grid approximation of the posterior is reused. In this way, the current posterior can be approximated accurately with few expensive, finer model discretizations. We point out that sparse grid approximations are based on point sequences in one dimension. However, starting with the second level the posterior densities are in general not separable and hence we cannot rely on a simple tensorization of univariate Leja points. Instead we construct Leja points w.r.t. a *Gaussian approximation* of the posterior, which is separable, and we then correct the bias introduced by this approximation in quadrature computations.

The remainder of this paper is structured as follows. In section 2 we provide the necessary background information. In particular, in subsection 2.1 we formulate the Bayesian inverse problem and discuss the computation of posterior expectations by importance sampling. Subsection 2.2 reviews multilevel approaches, and subsection 2.4 discusses generalized sparse grids. Section 3 contains the major contribution of our work, the multilevel adaptive sparse Leja approximation to the posterior density in a Bayesian inverse problem. This method is independent of the specific implementation of the adaptive sparse grid approximations. Details on the used dimension-adaptive approximations are given in section 4. In section 5, we present numerical results, comparing our multilevel algorithm with sampling methods and the classical multilevel approach based on telescoping sums. Finally, section 6 offers concluding remarks.

2. Background.

2.1. Bayesian inversion. To begin we formulate the Bayesian inverse problem. Let $\mathbf{X} \subset \mathbb{R}^{N_{\text{sto}}}$ denote the parameter space and $\mathbf{Y} = \mathbb{R}^{N_{\text{obs}}}$ be the data space. N_{sto} is the dimension of the data space, and N_{obs} is the number of observations. Notably, the parameter and data space are *finite-dimensional*. This allows us to work with densities w.r.t. the Lebesgue measure. The underlying mathematical model is formalized by a function $\mathcal{G} : \mathbf{X} \rightarrow \mathbf{Y}$, which maps from the parameter space to the data space. Noisy observations $\mathbf{y} \in \mathbf{Y}$ are obtained. To model the noise we assume that \mathbf{y} is a realization of the random variable $\mathcal{G}(\boldsymbol{\theta}^{\text{true}}) + \boldsymbol{\eta}$, where $\boldsymbol{\eta} \sim N(0, \Gamma)$ is nondegenerate Gaussian noise, and $\boldsymbol{\theta}^{\text{true}} \in \mathbf{X}$ is the true parameter. In an inverse problem we wish to identify the parameter $\boldsymbol{\theta}^{\text{true}}$, i.e., solve the equation

$$(2.1) \quad \mathcal{G}(\boldsymbol{\theta}) + \boldsymbol{\eta} = \mathbf{y}$$

for $\boldsymbol{\theta}$. This problem is typically ill-posed in the sense of Hadamard [19], due to noise, and since the low-dimensional data space is often not sufficiently rich to allow the identification of a unique parameter in the high-dimensional space \mathbf{X} . The ill-posedness can be cured, for example, by using deterministic regularization, such as Tikhonov regularization [21]. This approach, however, does not provide any probabilistic description of the inferred parameters $\boldsymbol{\theta}$ and thus no quantification of their uncertainty. To this end, we reformulate (2.1) as a Bayesian inverse problem. Next, we introduce our notation and briefly discuss Bayesian inversion, and we refer to [44] for more details.

We assume that $\boldsymbol{\theta}$ is an \mathbf{X} -valued random variable that is distributed according to a *prior measure* μ_0 with Lebesgue density π_0 on the parameter space \mathbf{X} . Moreover, we assume that $\boldsymbol{\theta}$ is stochastically independent of the noise $\boldsymbol{\eta}$. The density π_0 reflects our knowledge about $\boldsymbol{\theta}$ before we make an observation \mathbf{y} . The information provided by \mathbf{y} is modeled by the (data) likelihood. Since the noise $\boldsymbol{\eta}$ is Gaussian by assumption, the likelihood is given by

$$(2.2) \quad \begin{aligned} L(\boldsymbol{\theta}|\mathbf{y}) &:= \exp(-\Phi(\boldsymbol{\theta}; \mathbf{y})), \\ \Phi(\boldsymbol{\theta}; \mathbf{y}) &:= \frac{1}{2}\|\Gamma^{-1/2}(\mathbf{y} - \mathcal{G}(\boldsymbol{\theta}))\|^2. \end{aligned}$$

The function Φ is called potential or negative log-likelihood. The solution of the Bayesian inverse problem is the *posterior (measure)* $\mu^{\mathbf{y}}$, i.e., the conditional measure of $\boldsymbol{\theta}$ given that the event $\{\mathcal{G}(\boldsymbol{\theta}) + \boldsymbol{\eta} = \mathbf{y}\}$ occurred. The posterior measure $\mu^{\mathbf{y}}$ has also a density $\pi^{\mathbf{y}}$ which can be computed using Bayes's formula,

$$(2.3) \quad \begin{aligned} \pi^{\mathbf{y}}(\boldsymbol{\theta}) &= \frac{L(\boldsymbol{\theta}|\mathbf{y})\pi_0(\boldsymbol{\theta})}{Z(\mathbf{y})}, \quad \boldsymbol{\theta} \in X, \mathbf{y} \in Y, \\ Z(\mathbf{y}) &= \int_{\mathbf{X}} L(\boldsymbol{\theta}|\mathbf{y})\pi_0(\boldsymbol{\theta})d\boldsymbol{\theta}, \end{aligned}$$

provided that $0 < Z(\mathbf{y}) < \infty$. In the given setting (nondegenerate Gaussian additive noise, finite-dimensional data space), one can show that $Z(\mathbf{y})$ is always finite and bounded away from 0. This implies existence of the posterior measures; see [26]. The work [26] also establishes that Bayesian inverse problems of this type are always *well-posed*.

Finally, let $g : \mathbf{X} \rightarrow \mathbb{R}$ denote a quantity of interest (QoI) depending on the parameter $\boldsymbol{\theta}$. Since $\boldsymbol{\theta}$ is a random variable, one is typically interested in the forward propagation of uncertainties through the action of g . For instance, we wish to evaluate integrals of g w.r.t. the posterior measure:

$$(2.4) \quad \mathbb{E}_{\mu^{\mathbf{y}}}[g] = \int_{\mathbf{X}} g(\boldsymbol{\theta})\pi^{\mathbf{y}}(\boldsymbol{\theta})d\boldsymbol{\theta}.$$

In practice, we approximate integrals of this type via numerical quadrature. Note that we can write the expected value in (2.4) in terms of a ratio of two expected values w.r.t. the prior measure:

$$(2.5) \quad \mathbb{E}_{\mu^{\mathbf{y}}}[g] = \frac{1}{Z(\mathbf{y})} \int g(\boldsymbol{\theta})L(\boldsymbol{\theta}|\mathbf{y})\pi_0(\boldsymbol{\theta})d\boldsymbol{\theta} = \frac{\mathbb{E}_{\mu_0}[g(\cdot)L(\cdot|\mathbf{y})]}{\mathbb{E}_{\mu_0}[L(\cdot|\mathbf{y})]}.$$

Note that the prior is typically much more accessible compared to the posterior, via i.i.d. sampling or a closed form probability density function. If the two expected values in (2.5) are approximated with samples from μ_0 , we refer to this method by *importance sampling*. If the expected values are approximated with other numerical quadrature rules, e.g., quasi-Monte Carlo [38] or sparse grid quadrature [39, 41], we refer to any of these methods as *importance-sampling-based methods*.

2.2. Multilevel approximation of the quantity of interest. The approximation of the expected value $\mathbb{E}_{\mu^y}[g]$ involves two sources of error: (i) the quadrature error associated with the approximation of the measure μ^y , and (ii) the discretization error associated with the approximation of g . The quadrature error is typically controlled by the number of particles or grid points in the parameter domain. The discretization error in g is often controlled by the mesh size in the physical domain. In our setting, the evaluation of g typically involves a computationally expensive model, e.g., a PDE. If we wish to construct accurate approximations to $\mathbb{E}_{\mu^y}[g]$, then g has to be discretized with a high resolution on a fine grid in physical space, and g has to be evaluated for a large number of parameter values. For these reasons the approximation of $\mathbb{E}_{\mu^y}[g]$ is computationally demanding.

Multilevel methods provide a framework to approximate high-resolution problems efficiently by combining evaluations from fine and coarse grid approximations. Specifically, approximations based on quadrature and physical domain discretization grids of complementary resolution are combined such that most computations are done on coarse grids while fine grid approximations are evaluated only a limited number of times. In this way, the overall computational cost is reduced, while the accuracy is preserved. A large number of multilevel approaches for Bayesian inverse problems proceed by using a telescoping sum based on the linearity of the expectation operator; see, e.g., [9]. Alternatively, it is possible to construct a multilevel approximation without relying on such a telescoping sum. Examples are the multifidelity preconditioned MCMC method in [36], Multilevel Sequential² Monte Carlo [28], and our multilevel sparse Leja approximation presented in section 3.

2.3. Assumptions. We construct our proposed multilevel adaptive sparse grid Leja approach using sparse grids. Hence, we need the following two assumptions:

A1. The parameter space is a tensor product space, i.e.,

$$\mathbf{X} = \bigotimes_{i=1}^{N_{\text{sto}}} X_i,$$

where $X_i \subset \mathbb{R}$ for $i = 1, 2, \dots, N_{\text{sto}}$.

A2. The prior density π_0 has a product structure, i.e.,

$$(2.6) \quad \pi_0(\boldsymbol{\theta}) = \prod_{i=1}^{N_{\text{sto}}} \pi_{0,i}(\theta_i),$$

where $\pi_{0,i}: X_i \rightarrow \mathbb{R}$ are its marginals for $i = 1, 2, \dots, N_{\text{sto}}$.

Assumption A1 can always be satisfied by embedding a nontensorized parameter space into a hyperrectangle of suitable dimension. Assumption A2 is fulfilled if the components of $\boldsymbol{\theta}$ are stochastically independent under the prior measure. If assumption A2 is not satisfied, the Gaussian approximation of π_0 is needed (see section 3).

2.4. Approximation with generalized sparse grids. We aim to approximate posterior density functions with sparse grid interpolation and quadrature at each level

in our multilevel approach. To this end, we employ *generalized, adaptive Smolyak approximations* [42]. Smolyak's algorithm, also known as the combination scheme [18], is a strategy to construct multivariate sparse grid approximations by weakening the assumed coupling between the input dimensions (see, e.g., [6, 13]). We briefly summarize Smolyak's algorithm. For a more detailed overview of this approach and its application in scientific computing, see [2, 48] and the references therein.

Let $f^i : X_i \subset \mathbb{R} \rightarrow \mathbb{R}$ denote univariate functions, where $i = 1, 2, \dots, N_{\text{sto}}$. In addition, let $f^{N_{\text{sto}}} : \mathbf{X} \rightarrow \mathbb{R}$ denote a multivariate function with a scalar output. For example, $f^{N_{\text{sto}}}$ could be the potential function, $\Phi(\boldsymbol{\theta}; \mathbf{y})$, or the QoI, $g(\boldsymbol{\theta})$. Let $\mathcal{U}^i[f^i]$ for $i = 1, 2, \dots, N_{\text{sto}}$ denote either univariate interpolation or integration operators defined w.r.t. a weight function $w : X_i \rightarrow \mathbb{R}_+$, which in our context is the i th component of the prior density. Further, consider approximations $\mathcal{U}_k^i[f^i]$ that converge as $k \rightarrow \infty$, where k is typically referred to as *level*. Starting from one-dimensional (1D) difference or *hierarchical surplus operators*,

$$(2.7) \quad \Delta_k^i[f^i] := \mathcal{U}_k^i[f^i] - \mathcal{U}_{k-1}^i[f^i], \quad i = 1, 2, \dots, N_{\text{sto}},$$

with the convention $\Delta_1^i[f^i] := \mathcal{U}_1^i[f^i]$, Smolyak's approximation formula reads

$$(2.8) \quad \mathcal{U}_{\mathcal{K}}[f^{N_{\text{sto}}}] = \sum_{\mathbf{k} \in \mathcal{K}} \left(\Delta_{k_1}^1 \otimes \Delta_{k_2}^2 \otimes \dots \otimes \Delta_{k_{N_{\text{sto}}}}^{N_{\text{sto}}} \right) [f^{N_{\text{sto}}}] = \sum_{\mathbf{k} \in \mathcal{K}} \Delta_{\mathbf{k}}[f^{N_{\text{sto}}}],$$

where $\mathbf{k} := (k_1, k_2, \dots, k_{N_{\text{sto}}}) \in \mathbb{N}^{N_{\text{sto}}}$ is a *multi-index* and \mathcal{K} is a *finite set of multi-indices*. Note that by construction, (2.8) requires the underlying multivariate space, \mathbf{X} , as well as the corresponding weight function to be separable. When the weight function is a density the stochastic parameters need to be independent.

Since (2.8) is written in terms of tensorizations of univariate difference operators (2.7) the set \mathcal{K} must be constructed such that the summation in (2.8) telescopes correctly. Suitable sets of multi-indices \mathcal{K} are called *admissible* (or *downward closed*; see [17]). In particular, for an admissible set \mathcal{K} it holds that $\mathbf{k} \in \mathcal{K} \Rightarrow \mathbf{k} - \mathbf{e}_i \in \mathcal{K}$ for $i = 1, 2, \dots, N_{\text{sto}}$, where \mathbf{e}_i denotes the i th unit vector in $\mathbb{R}^{N_{\text{sto}}}$. To construct the approximations $\mathcal{U}_k^i[f^i]$, we employ *weighted (L)-Leja sequences* [22]. Let $\pi(\boldsymbol{\theta})$ be a density associated to the underlying multivariate space, \mathbf{X} . For example, this density can be the prior, π_0 , or the Gaussian approximation of the posterior which we use in our approach (see subsection 3.3). From assumption A1, $\pi(\boldsymbol{\theta})$ needs to have a product structure, i.e., $\pi(\boldsymbol{\theta}) = \prod_{i=1}^{N_{\text{sto}}} \pi_i(\theta_i)$, where $\pi_i : X_i \rightarrow [0, 1]$ are the marginal densities. We thus construct weighted (L)-Leja points recursively as

$$(2.9) \quad \begin{aligned} \theta_1 &= \operatorname{argmax}_{\theta \in X_i} \pi_i(\theta), \\ \theta_n &= \operatorname{argmax}_{\theta \in X_i} \pi_i(\theta) \prod_{m=1}^{n-1} |\theta - \theta_m|, \quad n = 2, 3, \dots \end{aligned}$$

When π_i is the standard uniform density with support $[0, 1]$, we choose $\theta_1 = 0.5$. Note that the above point sequence is in general not uniquely defined, because (2.9) might have multiple maximizers. In that case we simply pick one of the maximizers. Weighted (L)-Leja sequences allow the construction of sparse grid approximations for arbitrary probability densities. Moreover, they lead to accurate approximations with low cardinality. Let $m(k)$ denote the number of (L)-Leja points associated to level k , i.e., the *level-to-nodes* mapping. The construction (2.9) indicates that weighted (L)-Leja points form an interpolatory sequence, i.e., only one extra point is needed to

increase the interpolation degree by one. Thus, for interpolation, we employ a level-to-nodes mapping $m(k) = k$. Note that due to the nestedness of (L)-Leja sequences, $m(k) - m(k-1) = 1$. So as we increase the level, we need only one extra evaluation of the underling function. For quadrature, on the other hand, we use $m(k) = 2k-1$, i.e., we add two extra (L)-Leja points for all levels $k \geq 2$. This is because (2.9) puts the first (L)-Leja point in the middle of the domain, while the next two points are placed on the boundary of the weight function's support. In this way, adding only one (L)-Leja point at a time will lead to a zero quadrature weight at level $k=2$, causing the employed quadrature algorithms to stop prematurely.

To fully define (2.8), we need to specify the multi-index set \mathcal{K} as well. We construct \mathcal{K} adaptively based on the *dimension-adaptive* algorithm of [17, 20], which we outline in section 4.

3. Multilevel sparse Leja algorithm. This section contains the major contribution of our work. Our goal is to address the challenges of Bayesian inversion in computationally expensive problems. To this end, we formulate a deterministic, multilevel, sampling-free methodology based on adaptive sparse grid approximations in which we sequentially update the auxiliary reference density as the level in the multilevel hierarchy increases.

Most computations in Bayesian inversion involve evaluations of the forward operator, $\mathcal{G}(\boldsymbol{\theta})$, which in this paper is assumed to be computationally expensive. When a large number of such evaluations is needed, the corresponding computational cost is prohibitive. To reduce the cost, we employ multilevel approximations. At each level, we construct sparse grid surrogates of the potential function $\Phi(\boldsymbol{\theta}; \mathbf{y})$. Our motivation is twofold. First, evaluating $\Phi(\boldsymbol{\theta}; \mathbf{y})$ means evaluating the forward model, $\mathcal{G}(\boldsymbol{\theta})$ (see (2.2)), hence the computationally expensive part. Second, even if $\mathcal{G}(\boldsymbol{\theta})$ is vector valued, $\Phi(\boldsymbol{\theta}; \mathbf{y})$ is a scalar. Adaptive sparse grid approximations can be constructed for vector-valued functions; however, a separate adaptive approximation is usually needed for each output component, which can be infeasibly expensive. After the surrogate is obtained, all other single level operations, which typically involve integration, employ this surrogate, making them computationally cheap. In the following, we use the superscripts *in* and *qu* to specifically refer to interpolation and quadrature, respectively, whereas superscript *op* is used to refer to either of the two operations.

In this paper, the surrogates of the potential function are constructed via adaptive sparse grid interpolation, whereas all integration operations are performed using adaptive sparse grid quadrature. The specific implementations do not influence the formulation of our multilevel approach. Thus we assume we have two adaptive strategies, `AdaptSGInterp`(tol^{in} , K_{\max}^{in} , g , π) and `AdaptSGQuad`(tol^{qu} , K_{\max}^{qu} , g , π), which depend on a tolerance, tol^{op} . The other inputs are a maximum reachable sparse grid level, K_{\max}^{op} , the target function, g , and the density function w.r.t. which the approximation is performed, π . Note that specific implementations might have additional input arguments; however, the four inputs considered here are sufficient to illustrate these algorithms. The adaptive strategies are summarized in section 4.

3.1. General setup. Let $J > 1$, $J \in \mathbb{N}$, denote the number of *levels* in our multilevel formulation. Further, let $A \in \{\mathcal{G}, \Phi, L, Z, \pi^{\mathbf{y}}\}$ denote a generic quantity depending on both physical and stochastic parameters. Let $j = 1, 2, \dots, J$. By h_j we characterize the discretization of the physical domain of the forward response operator $\mathcal{G}(\boldsymbol{\theta})$, where h_1 is the coarsest and h_J the finest discretization level. Hence, by A_j we denote the semidiscrete approximation of A depending on h_j , whereas $A_{\delta j}$ denotes

either $A_j - A_{j-1}$ or A_j/A_{j-1} . In addition, tol_j^{op} denotes the tolerance employed in the adaptive sparse grid approximations of A_j such that

$$\text{tol}_1^{\text{op}} \leq \text{tol}_2^{\text{op}} \leq \cdots \leq \text{tol}_J^{\text{op}}.$$

Thus by $A_{j,s}$ we denote the sparse grid approximation of A_j depending on tol_s^{op} .

In our multilevel formulation, we determine $A_{j,J-j+1}$ for all $j = 1, 2, \dots, J$. To simplify the notation we use the subscript $\ell(j)$ to refer to $(h_j, \text{tol}_{J-j+1}^{\text{op}})$ and the subscript $\ell(\delta j)$ to denote approximations $A_{\ell(\delta j)} \approx A_{\delta j}$. Hence we refer to the *level* j in our multilevel approach by $\ell(j)$ or $\ell(\delta j)$. Note that levels are used to characterize both sparse grid and multilevel formulations. To avoid confusion, we will explicitly specify what is meant by level in each context.

3.2. Level $\ell(1)$. At $\ell(1)$ we compute the approximation $\Phi_{\ell(1)}(\boldsymbol{\theta}; \mathbf{y}) \approx \Phi_1(\boldsymbol{\theta}; \mathbf{y})$ using adaptive sparse grid interpolation w.r.t. the prior π_0 . This is possible since π_0 has a product structure by assumption A2; see (2.6). The potential's approximation $\Phi_{\ell(1)}(\boldsymbol{\theta}; \mathbf{y})$ is used for $L_1(\boldsymbol{\theta}|\mathbf{y}) \approx L_{\ell(1)}(\boldsymbol{\theta}|\mathbf{y}) := \exp(-\Phi_{\ell(1)}(\boldsymbol{\theta}; \mathbf{y}))$, the level one likelihood surrogate. Afterward, we employ $L_{\ell(1)}(\boldsymbol{\theta}|\mathbf{y})$ to compute the evidence $Z_{\ell(1)}(\mathbf{y}) \approx Z_1(\mathbf{y})$ via adaptive sparse grid quadrature w.r.t. the prior density π_0 . Having computed $L_{\ell(1)}(\boldsymbol{\theta}|\mathbf{y})$ and $Z_{\ell(1)}(\mathbf{y})$ we apply formula (2.3) and obtain the posterior at level $\ell(1)$, $\pi_{\ell(1)}^{\mathbf{y}}(\boldsymbol{\theta})$. In addition, we also compute the posterior expectation, $\mathbf{m}_{\ell(1)} \in \mathbb{R}^{N_{\text{sto}}}$, where for $i = 1, 2, \dots, N_{\text{sto}}$,

$$\mathbf{m}_{\ell(1)}^i := Z_{\ell(1)}^{-1}(\mathbf{y}) \int_{\mathbf{X}} \theta_i L_{\ell(1)}(\boldsymbol{\theta}|\mathbf{y}) \pi_0(\boldsymbol{\theta}) d\boldsymbol{\theta},$$

and covariance matrix, $\mathbf{C}_{\ell(1)} \in \mathbb{R}^{N_{\text{sto}} \times N_{\text{sto}}}$, where for $i_1, i_2 = 1, 2, \dots, N_{\text{sto}}$,

$$\mathbf{C}_{\ell(1)}^{i_1 i_2} := Z_{\ell(1)}^{-1}(\mathbf{y}) \int_{\mathbf{X}} \theta_{i_1} \theta_{i_2} L_{\ell(1)}(\boldsymbol{\theta}|\mathbf{y}) \pi_0(\boldsymbol{\theta}) d\boldsymbol{\theta} - \mathbf{m}_{\ell(1)}^{i_1} \mathbf{m}_{\ell(1)}^{i_2},$$

which we need to construct the *Gaussian approximation* $\hat{\pi}_{\ell(1)}^{\mathbf{y}}(\boldsymbol{\theta}) := \mathcal{N}(\mathbf{m}_{\ell(1)}, \mathbf{C}_{\ell(1)})$ of $\pi_{\ell(1)}^{\mathbf{y}}(\boldsymbol{\theta})$ at the second level $\ell(2)$ (see subsection 3.3.1).

These steps are summarized in Algorithm 3.1. The first three inputs are the spatial discretization parameter h_1 and the tolerances for sparse grid interpolation and quadrature, tol_j^{in} and tol_j^{qu} . Moreover, $\mathbf{K}_{\max} := (K_{\max}^{\text{in}}, K_{\max}^{\text{qu}})$ comprises the maximum attainable sparse grid levels for the two adaptive operations. The last two inputs are the potential function, $\Phi(\boldsymbol{\theta}; \mathbf{y})$, and the prior density, $\pi_0(\boldsymbol{\theta})$.

Before explaining how our proposed approach proceeds at levels $\ell(j)$ with $j \geq 2$, we make the following remark.

Remark 3.1. When the underlying posterior density is concentrated in the support of the prior, adaptive sparse grid quadrature w.r.t. the prior typically fails to converge since most sparse grid points are placed outside of the region of high (and concentrated) posterior probability. Thus, the adaptive quadrature at level $\ell(1)$ in our proposed approach would fail to provide a Gaussian auxiliary reference density. Possible remedies include using a static sparse grid of a large enough level to ensure that grid points are placed within the region of high posterior probability (see also subsection 5.4). When using nested point sets, this task is not too difficult since computations from previous levels can be reused when the sparse grid level is increased. In the same direction, another remedy is to first compute approximations using a static sparse grid such that grid points are placed inside or close to the region of high

Algorithm 3.1 Level one adaptive sparse Leja algorithm for Bayesian inversion.

```

1: procedure LEVEL1SPARSELEJA( $h_1, tol_J^{\text{in}}, tol_J^{\text{qu}}, K_{\max}, \Phi(\boldsymbol{\theta}; \mathbf{y}), \pi_0(\boldsymbol{\theta})$ )
2:   Compute the potential's surrogate via adaptive sparse grid interpolation

$$\Phi_{\ell(1)}(\boldsymbol{\theta}; \mathbf{y}) = \text{AdaptSGInterp}(tol_J^{\text{in}}, K_{\max}^{\text{in}}, \Phi_1, \pi_0)$$

3:   Construct the likelihood surrogate  $L_{\ell(1)}(\boldsymbol{\theta}|\mathbf{y}) := \exp(-\Phi_{\ell(1)}(\boldsymbol{\theta}; \mathbf{y}))$ 
4:   Compute the evidence via adaptive sparse grid quadrature

$$Z_{\ell(1)}(\mathbf{y}) = \text{AdaptSGQuad}(tol_J^{\text{qu}}, K_{\max}^{\text{qu}}, L_{\ell(1)}, \pi_0)$$

5:   Compute the posterior

$$\pi_{\ell(1)}^{\mathbf{y}}(\boldsymbol{\theta}) := \frac{\pi_0(\boldsymbol{\theta})L_{\ell(1)}(\boldsymbol{\theta}|\mathbf{y})}{Z_{\ell(1)}(\mathbf{y})}$$

6:   Compute the expectation  $\mathbf{m}_{\ell(1)}$  of  $\pi_{\ell(1)}^{\mathbf{y}}(\boldsymbol{\theta})$  w.r.t.  $\pi_0(\boldsymbol{\theta})$ 
7:   Compute the covariance  $\mathbf{C}_{\ell(1)}$  of  $\pi_{\ell(1)}^{\mathbf{y}}(\boldsymbol{\theta})$  w.r.t.  $\pi_0(\boldsymbol{\theta})$ 
8:   return  $\pi_{\ell(1)}^{\mathbf{y}}(\boldsymbol{\theta}), \mathbf{m}_{\ell(1)}, \mathbf{C}_{\ell(1)}$ 
9: end procedure
```

posterior probability, and then to start the adaptive refining from this approximation. However, it is rather unclear how to choose the level of the initial grid and when to start the refinement process. Other solutions include employing a Laplace approximation of the posterior around the MAP point [5], which was proven to be a suitable choice in high-dimensional settings. Moreover, using tempering (see, e.g., [10]) or sparse grids with local (spatial) adaptivity [31] could also be alternative ways to alleviate the challenges of dealing with concentrated posteriors.

3.3. Level $\ell(j)$ with $j \geq 2$.

3.3.1. Gaussian approximation. At levels $\ell(j)$ with $j \geq 2$, we sequentially update the auxiliary reference density such that the previous level posterior, $\pi_{\ell(j-1)}^{\mathbf{y}}(\boldsymbol{\theta})$, is used as the prior; we detail the sequential update in subsection 3.3.2. To be able to construct sparse grid approximations w.r.t. $\pi_{\ell(j-1)}^{\mathbf{y}}(\boldsymbol{\theta})$, the underlying stochastic space needs to have a separable density (recall assumption A2). However, $\pi_{\ell(j-1)}^{\mathbf{y}}(\boldsymbol{\theta})$ is usually not separable. Therefore, we approximate $\pi_{\ell(j-1)}^{\mathbf{y}}(\boldsymbol{\theta})$ with a density $\hat{\pi}_{\ell(j-1)}^{\mathbf{y}}(\boldsymbol{\theta})$ that allows us to obtain the required product structure. In this paper, we approximate $\pi_{\ell(j-1)}^{\mathbf{y}}(\boldsymbol{\theta})$ with the Gaussian density $\hat{\pi}_{\ell(j-1)}^{\mathbf{y}}(\boldsymbol{\theta})$ defined as

$$(3.1) \quad \hat{\pi}_{\ell(j-1)}^{\mathbf{y}}(\boldsymbol{\theta}) := N(\mathbf{m}_{\ell(j-1)}, \mathbf{C}_{\ell(j-1)}),$$

where $\mathbf{m}_{\ell(j-1)}$ and $\mathbf{C}_{\ell(j-1)}$ are the expectation and covariance matrix of $\pi_{\ell(j-1)}^{\mathbf{y}}(\boldsymbol{\theta})$.

In most cases $\mathbf{C}_{\ell(j-1)}$ is not diagonal, i.e., $\hat{\pi}_{\ell(j-1)}^{\mathbf{y}}(\boldsymbol{\theta})$ does not have a product structure. Nevertheless, from the spectral decomposition $\mathbf{C}_{\ell(j-1)} = VDV^{-1}$, we have $\mathbf{C}_{\ell(j-1)}^{1/2} = VD^{1/2}V^{-1}$. We arrive at

$$(3.2) \quad \boldsymbol{\theta} = T_{\ell(j-1)}(\boldsymbol{\zeta}) := \mathbf{m}_{\ell(j-1)} + \mathbf{C}_{\ell(j-1)}^{1/2}\boldsymbol{\zeta} \Rightarrow \boldsymbol{\theta} \sim N(\mathbf{m}_{\ell(j-1)}, \mathbf{C}_{\ell(j-1)}),$$

where $\boldsymbol{\zeta}$ is a standard Gaussian random variable, i.e., $\boldsymbol{\zeta} \sim N(\mathbf{0}, I)$.

Formula (3.2) allows us to write a general multivariate Gaussian random variable with correlated components as a mapping of a standard multivariate Gaussian random variable, which has the desired product structure since the components of ζ are uncorrelated and thus independent. In our context, we use (3.2) as follows. We first generate 1D (L)-Leja points weighted w.r.t. the standard normal density, that is, $w(\theta) := \exp(-\theta^2/2)/\sqrt{2\pi}$ in (2.9). For quadrature, we compute 1D (L)-Leja quadrature weights w.r.t. normalized Hermite polynomials. That is, the quadrature weights are the first row of the inverse of the Vandermonde matrix obtained by evaluating Hermite polynomials at the underlying (L)-Leja points. We extend these constructions to N_{sto} dimensions via tensorization and employ (3.2) to obtain the desired weighted (L)-Leja points. Note that $T_{\ell(j-1)}$ in (3.2) is an *affine transport map* (see [32]).

3.3.2. Level update on tensor domain. We assume that $\pi_{\ell(j-1)}^{\mathbf{y}}(\boldsymbol{\theta})$ for $j \geq 2$ is not separable, hence we employ the Gaussian approximation (3.2) for all adaptive sparse grid operations; if $\pi_{\ell(j-1)}^{\mathbf{y}}(\boldsymbol{\theta})$ is separable, everything that follows is computed directly using $\pi_{\ell(j-1)}^{\mathbf{y}}(\boldsymbol{\theta})$ for all levels greater than two. Thus, we sequentially update the reference density in Bayes' formula (2.3) such that we reuse the Gaussian approximation of the posterior from the previous level, i.e.,

$$\begin{aligned} \pi_j^{\mathbf{y}}(\boldsymbol{\theta}) &:= \frac{L_j(\boldsymbol{\theta}|\mathbf{y})\pi_0(\boldsymbol{\theta})}{Z_j(\mathbf{y})} = \frac{L_j(\boldsymbol{\theta}|\mathbf{y})\pi_0(\boldsymbol{\theta})}{Z_j(\mathbf{y})} \frac{L_{j-1}(\boldsymbol{\theta}|\mathbf{y})}{L_{j-1}(\boldsymbol{\theta}|\mathbf{y})} \frac{Z_{j-1}(\mathbf{y})}{Z_{j-1}(\mathbf{y})} \\ (3.3) \quad &= \frac{L_{j-1}(\boldsymbol{\theta}|\mathbf{y})\pi_0(\boldsymbol{\theta})}{Z_{j-1}(\mathbf{y})} \frac{L_j(\boldsymbol{\theta}|\mathbf{y})}{L_{j-1}(\boldsymbol{\theta}|\mathbf{y})} \frac{Z_{j-1}(\mathbf{y})}{Z_j(\mathbf{y})} = \frac{\pi_{j-1}^{\mathbf{y}}(\boldsymbol{\theta}) \frac{L_j(\boldsymbol{\theta}|\mathbf{y})}{L_{j-1}(\boldsymbol{\theta}|\mathbf{y})}}{\frac{Z_j(\mathbf{y})}{Z_{j-1}(\mathbf{y})}} \\ &\approx \frac{\pi_{\ell(j-1)}^{\mathbf{y}}(\boldsymbol{\theta})L_{\delta j}(\boldsymbol{\theta}|\mathbf{y})}{Z_{\delta j}(\mathbf{y})} = \frac{\widehat{\pi}_{\ell(j-1)}^{\mathbf{y}}(\boldsymbol{\theta})L_{\delta j}(\boldsymbol{\theta}|\mathbf{y}) \frac{\pi_{\ell(j-1)}^{\mathbf{y}}(\boldsymbol{\theta})}{\widehat{\pi}_{\ell(j-1)}^{\mathbf{y}}(\boldsymbol{\theta})}}{Z_{\delta j}(\mathbf{y})}, \end{aligned}$$

where $L_{\delta j}(\mathbf{y}) := L_j(\mathbf{y})/L_{j-1}(\mathbf{y})$ and $Z_{\delta j}(\mathbf{y}) := Z_j(\mathbf{y})/Z_{j-1}(\mathbf{y})$. Note that in (3.3) we correct the bias introduced by the Gaussian approximation of the posterior from the previous level, $\widehat{\pi}_{\ell(j-1)}^{\mathbf{y}}$, with the ratio $\pi_{\ell(j-1)}^{\mathbf{y}}/\widehat{\pi}_{\ell(j-1)}^{\mathbf{y}}$.

First, we construct an adaptive sparse grid interpolation surrogate $\Phi_{\ell(\delta j)}(\boldsymbol{\theta}; \mathbf{y})$ of $\Phi_{\delta j}(\boldsymbol{\theta}; \mathbf{y}) := \Phi_j(\boldsymbol{\theta}; \mathbf{y}) - \Phi_{j-1}(\boldsymbol{\theta}; \mathbf{y})$ w.r.t. the density $\widehat{\pi}_{\ell(j-1)}^{\mathbf{y}}(\boldsymbol{\theta})$ because it holds that

$$L_{\delta j}(\boldsymbol{\theta}|\mathbf{y}) := \frac{\exp(-\Phi_j(\boldsymbol{\theta}; \mathbf{y}))}{\exp(-\Phi_{j-1}(\boldsymbol{\theta}; \mathbf{y}))} = \exp(-\Phi_{\delta j}(\boldsymbol{\theta}; \mathbf{y})).$$

Recall that the mapping $T_{\ell(j-1)}$ defined in (3.2) allows us to use adaptive sparse grid interpolation w.r.t. the Gaussian approximation $\widehat{\pi}_{\ell(j-1)}^{\mathbf{y}}(\boldsymbol{\theta})$. To construct the surrogate for the potential function $\Phi_{\delta j}(\boldsymbol{\theta}; \mathbf{y})$ we employ $T_{\ell(j-1)}$ and obtain

$$\Phi_{\delta j}(\boldsymbol{\theta}; \mathbf{y}) \approx \Phi_{\ell(\delta j)}(T_{\ell(j-1)}(\boldsymbol{\zeta}); \mathbf{y}).$$

$\Phi_{\ell(\delta j)}$ gives the approximation $L_{\ell(\delta j)}(T_{\ell(j-1)}(\boldsymbol{\zeta})|\mathbf{y}) := \exp(-\Phi_{\ell(\delta j)}(T_{\ell(j-1)}(\boldsymbol{\zeta}); \mathbf{y}))$.

We explain next how quadrature operations are performed starting with level $\ell(2)$. To this end, we first prove the following lemma. Let

$$\pi_G(\boldsymbol{\zeta}) := N(\mathbf{0}, I) = \frac{\exp(-\frac{1}{2}\boldsymbol{\zeta}^T \boldsymbol{\zeta})}{\sqrt{(2\pi)^{N_{\text{sto}}}}}$$

denote the standard multivariate normal density. Recall the Gaussian auxiliary density $\widehat{\pi}_{\ell(j-1)}^{\mathbf{y}}$ defined in (3.1) and the mapping $T_{\ell(j-1)}(\boldsymbol{\zeta}) = \mathbf{m}_{\ell(j-1)} + \mathbf{C}_{\ell(j-1)}^{1/2} \boldsymbol{\zeta}$ from (3.2).

LEMMA 3.2. *For an integrable function $g : \mathbf{X} \rightarrow \mathbb{R}$ we have that*

$$(3.4) \quad \int_{\mathbf{X}} g(\boldsymbol{\theta}) \hat{\pi}_{\ell(j-1)}^{\mathbf{y}}(\boldsymbol{\theta}) d\boldsymbol{\theta} = \int_{\mathbb{R}^{N_{\text{sto}}} \times \mathbb{R}^{d_{\text{sto}}}} g(T_{\ell(j-1)}(\boldsymbol{\zeta})) \pi_G(\boldsymbol{\zeta}) d\boldsymbol{\zeta}.$$

Proof. $T_{\ell(j-1)}$ is injective and differentiable with Jacobian $DT_{\ell(j-1)}(\boldsymbol{\zeta}) = \mathbf{C}_{\ell(j-1)}^{1/2}$ which is nonzero for all $\boldsymbol{\zeta}$ (recall (3.2)). From $\boldsymbol{\theta} = T_{\ell(j-1)}(\boldsymbol{\zeta}) = \mathbf{m}_{\ell(j-1)} + \mathbf{C}_{\ell(j-1)}^{1/2} \boldsymbol{\zeta}$,

$$d\boldsymbol{\theta} = |\det(DT_{\ell(j-1)})(\boldsymbol{\zeta})| d\boldsymbol{\zeta} = \det(\mathbf{C}_{\ell(j-1)}^{1/2}) d\boldsymbol{\zeta}.$$

Thus, if we make the substitution $\boldsymbol{\theta} = T_{\ell(j-1)}(\boldsymbol{\zeta})$ in $\int_{\mathbf{X}} g(\boldsymbol{\theta}) \hat{\pi}_{\ell(j-1)}^{\mathbf{y}}(\boldsymbol{\theta}) d\boldsymbol{\theta}$, we obtain

$$(3.5) \quad \int_{\mathbf{X}} g(\boldsymbol{\theta}) \hat{\pi}_{\ell(j-1)}^{\mathbf{y}}(\boldsymbol{\theta}) d\boldsymbol{\theta} = \int_{\mathbb{R}^{N_{\text{sto}}} \times \mathbb{R}^{d_{\text{sto}}}} g(T_{\ell(j-1)}(\boldsymbol{\zeta})) \hat{\pi}_{\ell(j-1)}^{\mathbf{y}}(T_{\ell(j-1)}(\boldsymbol{\zeta})) \det(\mathbf{C}_{\ell(j-1)}^{1/2}) d\boldsymbol{\zeta}.$$

In the next step, we analyze the product $\hat{\pi}_{\ell(j-1)}^{\mathbf{y}}(T_{\ell(j-1)}(\boldsymbol{\zeta})) \det(\mathbf{C}_{\ell(j-1)}^{1/2})$ using (3.2):

$$(3.6) \quad \begin{aligned} \hat{\pi}_{\ell(j-1)}^{\mathbf{y}}(T_{\ell(j-1)}(\boldsymbol{\zeta})) \det(\mathbf{C}_{\ell(j-1)}^{1/2}) &= \hat{\pi}_{\ell(j-1)}^{\mathbf{y}}(\mathbf{m}_{\ell(j-1)} + \mathbf{C}_{\ell(j-1)}^{1/2} \boldsymbol{\zeta}) \det(\mathbf{C}_{\ell(j-1)}^{1/2}) \\ &= \frac{\exp(-\frac{1}{2} \boldsymbol{\zeta}^T \boldsymbol{\zeta})}{\sqrt{(2\pi)^{N_{\text{sto}}} \det(\mathbf{C}_{\ell(j-1)})}} \det(\mathbf{C}_{\ell(j-1)}^{1/2}) \\ &= \frac{\exp(-\frac{1}{2} \boldsymbol{\zeta}^T \boldsymbol{\zeta})}{\sqrt{(2\pi)^{N_{\text{sto}}}}} = \pi_G(\boldsymbol{\zeta}), \end{aligned}$$

where we used $\sqrt{\det(\mathbf{C}_{\ell(j-1)})} = \det(\mathbf{C}_{\ell(j-1)}^{1/2})$ because $\mathbf{C}_{\ell(j-1)}$ is a covariance matrix, hence symmetric and positive definite. From (3.5) and (3.6) we thus get

$$\int_{\mathbf{X}} g(\boldsymbol{\theta}) \hat{\pi}_{\ell(j-1)}^{\mathbf{y}}(\boldsymbol{\theta}) d\boldsymbol{\theta} = \int_{\mathbb{R}^{N_{\text{sto}}} \times \mathbb{R}^{d_{\text{sto}}}} g(T_{\ell(j-1)}(\boldsymbol{\zeta})) \pi_G(\boldsymbol{\zeta}) d\boldsymbol{\zeta}.$$

□

Therefore, the mapping $T_{\ell(j-1)}(\boldsymbol{\zeta})$ leads to integration w.r.t. the standard multivariate Gaussian density π_G .

To evaluate the ratio of evidence $Z_{\delta j}(\mathbf{y})$ we make use of the sequential update formula (3.3) and Lemma 3.2, in which we also employ the bias correcting ratio $\pi_{\ell(j-1)}^{\mathbf{y}} / \hat{\pi}_{\ell(j-1)}^{\mathbf{y}}$ to obtain

$$(3.7) \quad \begin{aligned} Z_{\delta j}(\mathbf{y}) &= \int_{\mathbf{X}} \hat{\pi}_{\ell(j-1)}^{\mathbf{y}}(\boldsymbol{\theta}) L_{\delta j}(\boldsymbol{\theta} | \mathbf{y}) \frac{\pi_{\ell(j-1)}^{\mathbf{y}}(\boldsymbol{\theta})}{\hat{\pi}_{\ell(j-1)}^{\mathbf{y}}(\boldsymbol{\theta})} d\boldsymbol{\theta} \\ &\approx \int_{\mathbb{R}^{d_{\text{sto}}}} L_{\ell(\delta j)}(T_{\ell(j-1)}(\boldsymbol{\zeta}) | \mathbf{y}) \frac{\pi_{\ell(j-1)}^{\mathbf{y}}(T_{\ell(j-1)}(\boldsymbol{\zeta}))}{\hat{\pi}_{\ell(j-1)}^{\mathbf{y}}(T_{\ell(j-1)}(\boldsymbol{\zeta}))} \pi_G(\boldsymbol{\zeta}) d\boldsymbol{\zeta}. \end{aligned}$$

Therefore, to obtain the evidence approximation $Z_{\ell(\delta j)}(\mathbf{y}) \approx Z_{\delta j}(\mathbf{y})$, we numerically integrate $(L_{\ell(\delta j)} \pi_{\ell(j-1)}^{\mathbf{y}} / \hat{\pi}_{\ell(j-1)}^{\mathbf{y}}) \circ T_{\ell(j-1)}$ w.r.t. the density π_G via adaptive sparse grid quadrature. For all other quadrature computations, for example, the assessment of the mean and covariance of the posterior densities or the computation of the QoI, we employ Lemma 3.2. Note that in this way, we perform the multilevel decomposition implicitly, different from standard multilevel methods in which the QoI is assessed explicitly via telescoping sums. Moreover, at the end of our multilevel algorithm we also obtain a surrogate for the posterior density which can be further used, for example, in an uncertainty propagation setting.

We summarize the steps for levels greater than two in Algorithm 3.2. The first three inputs are the number of levels, J , the sequence of mesh sizes, \mathbf{h} , and \mathbf{tol} ,

Algorithm 3.2 Multilevel adaptive sparse Leja algorithm.

```

1: procedure MULTILEVELADAPTSPARSELEJA( $J, \mathbf{h}, \mathbf{tol}, \mathbf{K}_{\max}, \Phi(\boldsymbol{\theta}; \mathbf{y}), \pi_0(\boldsymbol{\theta}), g$ )
2:   Use Algorithm 3.1 to obtain

 $\pi_{\ell(1)}^{\mathbf{y}}(\boldsymbol{\theta}), \mathbf{m}_{\ell(1)}, \mathbf{C}_{\ell(1)} = \text{Level1SparseLeja}(h_1, tol_J^{\text{in}}, tol_J^{\text{qu}}, \mathbf{K}_{\max}, \Phi, \pi_0)$ 

3:   for  $j \leftarrow 2, J$  do
4:     Construct the Gaussian approximation (3.1) and the mapping (3.2)

 $\hat{\pi}_{\ell(j-1)}^{\mathbf{y}}(\boldsymbol{\theta}) := N(\mathbf{m}_{\ell(j-1)}, \mathbf{C}_{\ell(j-1)}), \quad T_{\ell(j-1)}(\zeta) := \mathbf{m}_{\ell(j-1)} + \mathbf{C}_{\ell(j-1)}^{1/2} \zeta$ 

5:     Compute the potentials ratio surrogate via adaptive interpolation

 $\Phi_{\ell(\delta j)}(\boldsymbol{\theta}; \mathbf{y}) = \text{AdaptSGInterp}\left(tol_{J-j+1}^{\text{in}}, K_{\max}^{\text{in}}, \Phi_{\delta j} \circ T_{\ell(j-1)}(\zeta), \hat{\pi}_{\ell(j-1)}^{\mathbf{y}}\right)$ 

6:     Construct  $L_{\ell(\delta j)}(T_{\ell(j-1)}(\zeta) | \mathbf{y}) := \exp(-\Phi_{\ell(\delta j)}(T_{\ell(j-1)}(\zeta); \mathbf{y}))$ 
7:     Compute the evidence ratio via adaptive quadrature

 $Z_{\ell(\delta j)}(\mathbf{y}) = \text{AdaptSGQuad}\left(tol_{J-j+1}^{\text{qu}}, K_{\max}^{\text{qu}}, L_{\ell(\delta j)}, \hat{\pi}_{\ell(j-1)}^{\mathbf{y}}\right)$ 

8:     Compute the updated posterior

 $\pi_{\ell(j)}^{\mathbf{y}}(\boldsymbol{\theta}) := \frac{\pi_{\ell(j-1)}^{\mathbf{y}}(\boldsymbol{\theta}) L_{\ell(\delta j)}(\boldsymbol{\theta} | \mathbf{y})}{Z_{\ell(\delta j)}(\mathbf{y})}$ 

9:     Compute the expectation  $\mathbf{m}_{\ell(j)}$  of  $\pi_{\ell(j)}^{\mathbf{y}}(\boldsymbol{\theta})$  w.r.t.  $\hat{\pi}_{\ell(j-1)}^{\mathbf{y}}(T_{\ell(j-1)}(\zeta))$ 
10:    Compute the covariance  $\mathbf{C}_{\ell(j)}$  of  $\pi_{\ell(j)}^{\mathbf{y}}(\boldsymbol{\theta})$  w.r.t.  $\hat{\pi}_{\ell(j-1)}^{\mathbf{y}}(T_{\ell(j-1)}(\zeta))$ 
11:    end for
12:    Compute  $g_{\ell(J)} \approx g$  and integrate w.r.t.  $\pi_{\ell(J)}^{\mathbf{y}} \rightarrow \mathcal{I}_{\ell(J)}$ 
13:    return  $\mathcal{I}_{\ell(J)}$ 
14: end procedure

```

which comprises the tolerances for adaptive sparse grid interpolation and quadrature at all levels. The next input denotes the maximum reachable levels for the adaptive algorithms, $\mathbf{K}_{\max} := (K_{\max}^{\text{qu}}, K_{\max}^{\text{in}})$. Finally, π_0 is the prior density, $\Phi(\boldsymbol{\theta}; \mathbf{y})$ is the potential function, and g is the QoI. We combine Algorithms 3.1 and 3.2 and depict all steps in our proposed multilevel approach in Figure 1.

3.4. Computational cost. The largest computational effort in the proposed multilevel methodology is spent in finding the interpolation surrogates since this involves evaluations of the forward operator. Thus, for $j = 1, 2, \dots, J$, let C_{h_j} denote the cost of the evaluating once the forward model is discretized using a mesh depending on h_j . Additionally, let $N_{tol_{J-j+1}^{\text{in}}}$ denote the number of forward operator solves to achieve tolerance tol_{J-j+1}^{in} for adaptive sparse interpolation. Then, the *total interpolation cost* of our approach reads

$$\text{cost}_{\text{MLSL}}^{\text{in}} = \sum_{j=1}^{J-1} \left(N_{tol_{J-j+1}^{\text{in}}} + N_{tol_{J-j}^{\text{in}}} \right) C_{h_j} + N_{tol_1^{\text{in}}} C_{h_J}.$$

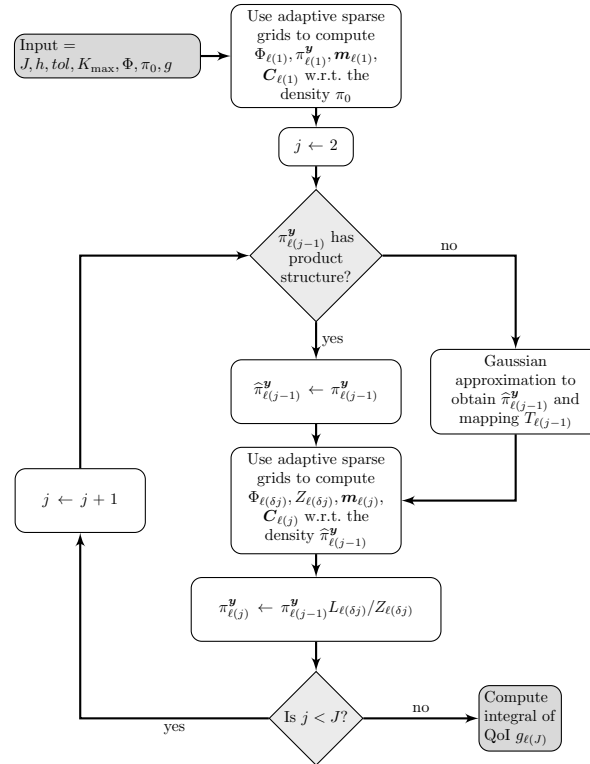


FIG. 1. Flowchart of the multilevel adaptive sparse Leja algorithm. The goal is to approximate the posterior density π^y and $\mathbb{E}_{\pi^y}[g]$ for an output QoI g at level J given the prior density π_0 .

We obtain the above number because for each level except the last one, the same potential function and thus the same forward model enter two different likelihood ratios (see (3.3)). Assuming that (i) Φ_{δ_j} is getting close to zero as j increases and (ii) the Gaussian approximation of the posterior from level $j - 1$ is accurate, we expect the number of forward model solves needed for interpolation to decrease significantly with the level.

All other costs are due to computations depending on the interpolation surrogates. These costs are, however, insignificant compared to the evaluation cost of a computationally expensive forward operator.

4. Dimension adaptivity with sparse grids. In this section we discuss the construction of the multi-index set \mathcal{K} used in the sparse grid approximations defined in subsection 2.4 via adaptive refinement. For interpolation we consider a standard adaptive strategy as well as an enhanced approach that employs directional variance information. For quadrature we employ a standard adaptive strategy. In the following, our notation is similar to [13].

4.1. Standard dimension-adaptive interpolation and quadrature. Adaptive refinement is preferred especially when the underlying problem has a richer structure, such as anisotropic coupling of the input parameters or lower intrinsic dimensionality—which is typically the case in most problems (see, e.g., [6, 13, 14, 49]). The standard strategy is based on the dimension-adaptive algorithm of [17, 20]. The algorithm is described, e.g., in [6, 17, 35]. We summarize only the basic idea below.

$\mathcal{K} = \{\mathbf{1}\}$ initially. Each refinement step is performed using the following principle: if a current multi-index contributes significantly to the approximation, its adjacent neighbors are likely to contribute as well. Therefore, the forward neighbors of the multi-index with the largest contribution are added to \mathcal{K} provided that \mathcal{K} remains admissible. The contribution of each \mathbf{k} is assessed via a *refinement indicator* $\epsilon(\mathbf{k})$, whose choice has a crucial impact on the performance of the adaptive algorithm. In addition, a surrogate for the global error indicator $\rho := \sum_{\mathbf{k} \in \mathcal{A}} \epsilon(\mathbf{k})$ is computed at the refinement step. The standard algorithm typically stops if $\rho < tol^{\text{op}}$ for a user-defined tolerance tol^{op} , if $\mathcal{A} = \emptyset$, or if a user-defined maximum level K_{\max}^{op} is reached.

We define

$$(4.1) \quad \epsilon(\mathbf{k}) := s^{\text{op}} (\Delta_{\mathbf{k}}^{\text{op}} [f^{N_{\text{sto}}}] / \delta N_{\mathbf{k}},$$

where s^{op} is a function depending on the multivariate surplus $\Delta_{\mathbf{k}}^{\text{op}}[f^{N_{\text{sto}}}]$ and $\delta N_{\mathbf{k}}$ is the number model evaluations needed to assess $\Delta_{\mathbf{k}}^{\text{op}}[f^{N_{\text{sto}}}]$. Note that $\delta N_{\mathbf{k}}$ penalizes subspaces with a large number of points.

For sparse grid quadrature, we consider

$$s^{\text{qu}} (\Delta_{\mathbf{k}}^{\text{qu}} [f^{N_{\text{sto}}}]) := \| \Delta_{\mathbf{k}}^{\text{qu}} [f^{N_{\text{sto}}}] \|_{L^1} = | \Delta_{\mathbf{k}}^{\text{qu}} [f^{N_{\text{sto}}}] |,$$

which is a surrogate for the local quadrature error. For sparse grid interpolation, we use

$$(4.2) \quad s^{\text{in}} (\Delta_{\mathbf{k}}^{\text{in}} [f^{N_{\text{sto}}}]) := \| \Delta_{\mathbf{k}}^{\text{in}} [f^{N_{\text{sto}}}] \|_{L^2}.$$

In [13], we showed that (4.2) yields the local variance contribution of the surplus to the total variance. Specifically, we (i) perform a mapping from the interpolation to pseudospectral projection basis corresponding to $\Delta_{\mathbf{k}}^{\text{in}}[f^{N_{\text{sto}}}]$ and (ii) we use the fact that the resulting pseudospectral coefficients can be used to assess the surplus variance in the underlying subspace.

4.2. Directional variance dimension-adaptive sparse interpolation. Dimension adaptivity based on error indicators such as (4.1) does not inherently distinguish between the individual input parameters. Since in most problems the input parameters are anisotropically coupled, we wish to exploit this structure and tune the adaptive process such that it stops refining directions that are rendered unimportant. This is particularly important in our proposed approach since we update the prior starting with level $\ell(2)$ and thus we have updated information about the model's stochastic input parameters. To this end, for sparse interpolation, we enhance the standard adaptive strategy such that we additionally compute a global measure of importance of each input parameter via *total directional variances*, and we stop refining the directions having insignificant total directional variances.

To enhance the standard adaptive approach for interpolation, we proceed analogously to [13, 49]. Specifically, we again perform a mapping from interpolation to pseudospectral projection, but this time we consider the interpolation contribution associated to the entire active set \mathcal{A} . After we obtain the equivalent pseudospectral coefficients, we use the equivalence [46] between pseudospectral expansions Sobol' decompositions [43] to obtain directional variance surpluses, that is,

$$\left\| \sum_{\mathbf{k} \in \mathcal{A}} \Delta_{\mathbf{k}}^{\text{in}} [f^{N_{\text{sto}}}] \right\|_{L^2}^2 = \Delta V_{\mathcal{A}}^0 + \sum_{i=1}^{N_{\text{sto}}} \Delta V_{\mathcal{A}}^i + \Delta V_{\mathcal{A}}^{\text{int}},$$

where $\Delta V_{\mathcal{A}}^0$ refers to the expectation contribution, $\Delta V_{\mathcal{A}}^i$ are surplus contributions to the variances corresponding to the N_{sto} inputs taken separately, and $\Delta V_{\mathcal{A}}^{\text{int}}$ refers to the variance surplus due to all possible interactions between the inputs.

We want to assess the global measure of importance for each stochastic input. To this end, we compute *total directional variance surpluses* as

$$\Delta V_{\mathcal{A}}^{i,\text{tot}} := \Delta V_{\mathcal{A}}^i + \Delta V_{\mathcal{A}}^{i,\text{int}},$$

where $\Delta V_{\mathcal{A}}^{i,\text{int}}$ denotes the variance surplus due to all interactions involving direction i . Note that certain components of $\Delta V_{\mathcal{A}}^{i,\text{int}}$ are typically added multiple times. For example, if direction i_1 interacts with direction i_2 , then the corresponding variance surplus is added to both $\Delta V_{\mathcal{A}}^{i_1,\text{tot}}$ and $\Delta V_{\mathcal{A}}^{i_2,\text{tot}}$. A large $\Delta V_{\mathcal{A}}^{i,\text{tot}}$ implies that the i th parameter is significant from a stochastic perspective. To this end, we prescribe N_{sto} user-defined *directional tolerances* $\tau^{\text{in}} := (\tau_1^2, \tau_2^2, \dots, \tau_{N_{\text{sto}}}^2)$ and ascertain the importance of each input directions by comparing $\Delta V_{\mathcal{A}}^{i,\text{tot}}$ with τ_i^2 for $i = 1, 2, \dots, N_{\text{sto}}$. When the stochastic direction i is rendered unimportant, we simply stop adding multi-indices whose i th component exceeds the maximum i th index in the current multi-index set \mathcal{K} . In this way, the algorithm preferentially refines the most important directions, thus decreasing the overall computational cost. When neither of the directional tolerances is met, the enhanced algorithm reduces to the standard approach in subsection 4.1.

5. Numerical experiments. In this section we present the numerical results obtained using our proposed multilevel approach for Bayesian inversion. Moreover, we also employ a standard multilevel approach in which the adaptive sparse grid approximations are performed w.r.t. the prior density at all levels. Moreover, since the most popular approaches in Bayesian inversion are sampling-based, we additionally employ MCMC. We note, however, that MCMC is rather used as a qualitative reference.

5.1. Simple quadrature showcase. In this test case we investigate the behaviour of weighted (L)-Leja points in integration problems of the form

$$(5.1) \quad \mathcal{I}(g) := \int g(\boldsymbol{\theta}) \pi^y(\boldsymbol{\theta}) d\boldsymbol{\theta},$$

where $g(\boldsymbol{\theta})$ is an integrable function and $\pi^y(\boldsymbol{\theta})$ is the posterior density; we outline the setup used to compute $\pi^y(\boldsymbol{\theta})$ below. We assess (5.1) via quadrature w.r.t. two different weight functions. In the first case, we employ a standard importance-sampling-based strategy (recall (2.5)). Specifically, adaptive sparse grid quadrature w.r.t. the prior density, $\pi_0(\boldsymbol{\theta})$, with tolerance $\text{tol}_{\pi_0}^{\text{qu}}$ is used:

$$(5.2) \quad \mathcal{I}(g) = \int g(\boldsymbol{\theta}) \frac{L(\boldsymbol{\theta}|y)\pi_0(\boldsymbol{\theta})}{Z(y)} d\boldsymbol{\theta} \approx Z_{N_{\text{pr}}}^{-1}(y) \left(\sum_{n=1}^{N_{\text{pr}}} g(\boldsymbol{\theta}_{n,\text{pr}}) L(\boldsymbol{\theta}_{n,\text{pr}}|y) w_{n,\text{pr}} \right),$$

where $\{\boldsymbol{\theta}_{n,\text{pr}}\}_{n=1}^{N_{\text{pr}}}$ are (L)-Leja nodes computed w.r.t. $\pi_0(\boldsymbol{\theta})$ and

$$Z_{N_{\text{pr}}}(y) = \sum_{n=1}^{N_{\text{pr}}} \boldsymbol{\theta}_{n,\text{pr}} L(\boldsymbol{\theta}_{n,\text{pr}}|y) w_{n,\text{pr}}.$$

In the second strategy, we compute (5.1) using our proposed approach. We integrate (5.1) numerically via adaptive sparse grid quadrature w.r.t. the Gaussian approximation $\hat{\pi}^y(\boldsymbol{\theta})$ of the posterior density (recall (3.1)), using a tolerance $\text{tol}_{\hat{\pi}^y}^{\text{qu}}$:

$$(5.3) \quad \begin{aligned} \mathcal{I}(g) &= \int g(\boldsymbol{\theta}) \frac{\pi^y(\boldsymbol{\theta})}{\hat{\pi}^y(\boldsymbol{\theta})} \hat{\pi}^y(\boldsymbol{\theta}) d\boldsymbol{\theta} = \int g(T(\zeta)) \frac{\pi^y(T(\zeta))}{\hat{\pi}^y(T(\zeta))} \pi_G(\zeta) d\zeta \\ &\approx \sum_{n=1}^{N_{\text{post}}} g(T(\zeta_{n,\text{post}})) \frac{\pi^y(T(\zeta_{n,\text{post}}))}{\hat{\pi}^y(T(\zeta_{n,\text{post}}))} w_{n,\text{post}}, \end{aligned}$$

where $\{\zeta_{n,\text{post}}\}_{n=1}^{N_{\text{post}}}$ are (L)-Leja nodes computed based on the standard multivariate normal density, π_G , and $T(\zeta) := \mathbf{m} + \mathbf{C}^{1/2}\zeta$, where \mathbf{m} and \mathbf{C} are the expectation and covariance matrix associated with the biasing density $\hat{\pi}^y(\boldsymbol{\theta})$.

We consider the following forward model:

$$\mathcal{G}(\boldsymbol{\theta}) := \frac{A(\theta_1)}{(w(\theta_2)\pi)^2} (\sin(w(\theta_2)\pi x) - \sin(w(\theta_2)\pi)x),$$

where $x \in [0, 1]$, $A(\theta_1) = 20\theta_1 + 1$, and $w(\theta_2) = \theta_2 + 1.2$. We employ Bayesian inversion to infer (θ_1, θ_2) . The prior is the uniform density in $[0, 1]^2$, i.e., $\pi_0 = U(0, 1)^2$. The observation data \mathbf{y} are generated synthetically using $(\theta_1, \theta_2)_{\text{true}} = (0.45, 0.65)$. We take $N_{\text{obs}} = 9$ measurements at locations $o_j = 0.1j$, $j = 1, 2, \dots, 9$, assumed to be corrupted by additive Gaussian noise $\eta \sim N(\mathbf{0}, 0.1^2 I)$. We depict the prior and posterior densities in the left figure in Figure 2. Observe that the posterior is unimodal and nonsymmetric, but it can be well approximated with a Gaussian density.

In the numerical experiments, we let $g(\boldsymbol{\theta}) := \exp(-\theta_1 - \theta_2)$ in (5.1). We compute a sampling solution using $3 \cdot 10^5$ Metropolis–Hastings MCMC (MH) samples obtained from a random walk Gaussian proposal with initial sample $\boldsymbol{\theta}_0 = (1, 1)$ and covariance matrix $C_{\text{MH}} = 7 \cdot 10^{-3} I$. The acceptance rate is 44%. Additionally, we employ a tolerance $\text{tol}_{\pi_0}^{\text{qu}} = 10^{-11}$ in (5.2) and a tolerance $\text{tol}_{\hat{\pi}^y}^{\text{qu}} = 10^{-5}$ in (5.3).

The results are summarized in Table 1. The employed tolerances in the two (L)-Leja sparse grid quadrature approaches are sufficient to match four digits of the MCMC results. However, integrating w.r.t. the prior requires 1603 nodes, whereas our approach which uses the Gaussian approximation of the posterior as weight function requires only 49 quadrature nodes, i.e., almost 33 times fewer points. This is because the support of the prior density, $\pi_0(\boldsymbol{\theta})$, is significantly larger than the support of the posterior: when integrating w.r.t. the prior density, the adaptive algorithm places a large number of quadrature points outside of the support of the posterior.

We visualize the quadrature nodes corresponding to (5.2) and (5.3) in the center and right figures in Figure 2, respectively.

Remark 5.1. Adaptive sparse grid quadrature w.r.t. an uninformative prior can sometimes stop early since the quadrature points will fall outside of the support of

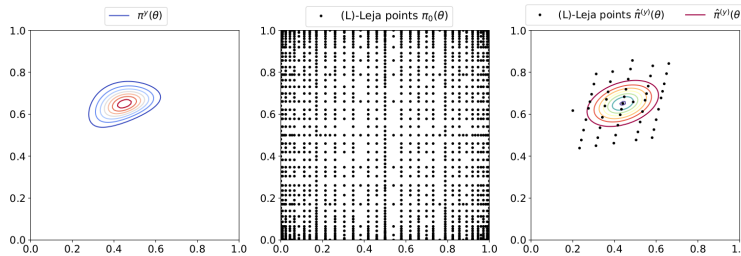


FIG. 2. Left: Posterior density $\pi^y(\boldsymbol{\theta})$. Center: (L)-Leja points computed w.r.t. the uniform prior density used in the integration problem (5.2). Right: Gaussian approximation $\hat{\pi}^y(\boldsymbol{\theta})$ of the posterior and the associated weighted (L)-Leja points used in (5.3).

TABLE 1

Results for the quadrature problem (5.1) using an MH solution with $3 \cdot 10^5$ samples, integration w.r.t. the prior density as in (5.2), and our proposed approach in which we integrate w.r.t. the Gaussian approximation of the posterior, as shown in (5.3).

Method	Number of quadrature points	Result
MH	$3 \cdot 10^5$	0.33813
Integration w.r.t. π_0	1603	0.33813
Integration w.r.t. $\hat{\pi}^y(\boldsymbol{\theta})$	49	0.33811

TABLE 2

Multilevel setup for the 2D inversion problem with forward model (5.4).

Level	h	tol^{in}	τ^{in}	tol^{qu}
$\ell(1)$	$h_1 = \sqrt{2}/2^4$	$tol_3^{in} = 10^{-5}$	$\tau_3^{in} = (10^{-7}, 10^{-7})$	$tol_3^{qu} = 10^{-12}$
$\ell(2)$	$h_2 = \sqrt{2}/2^5$	$tol_2^{in} = 10^{-4}$	$\tau_2^{in} = (10^{-6}, 10^{-6})$	$tol_2^{qu} = 10^{-11}$
$\ell(3)$	$h_3 = \sqrt{2}/2^6$	$tol_1^{in} = 10^{-3}$	$\tau_1^{in} = (10^{-5}, 10^{-5})$	$tol_1^{qu} = 10^{-10}$

the integrated function, yielding null evaluations and thus null error indicators. To overcome this, one could employ nonadaptive quadrature with a sufficiently large, a priori chosen number of nodes to cover the support of the integrated function.

5.2. Source inversion with one source in a 2D spatial domain. Consider a 2D Bayesian inverse problem in which the forward model $\mathcal{G}(\boldsymbol{\theta})$ is an elliptic PDE defined on $\Omega := [0, 1]^2$,

$$(5.4) \quad \begin{aligned} -(u_{xx} + u_{yy})(x, y) &= A(\alpha) \exp(-[(x - \theta_1)^2 + (y - \theta_2)^2]/2\alpha^2), & (x, y) \in \Omega, \\ u(x, y) &= 0, & (x, y) \in \partial\Omega, \end{aligned}$$

with $A(\alpha) = 5/(2\pi\alpha^2)$ and $\alpha = 0.2$.

The goal is to infer the coordinates (θ_1, θ_2) of the source term in the right-hand side, i.e., we seek the solution to a source inversion problem. We perform the multilevel Bayesian inversion as described in Algorithms 3.1 and 3.2 with three levels, i.e., $J = 3$. Thus $j = 1, 2, 3$. The employed multilevel setup is summarized in Table 2. Standard triangular FEs with mesh widths h_j are used for spatial discretization. To find surrogates for the potential function at each level in our proposed multilevel approach we employ both adaptive sparse interpolation variants summarized in section 4. Recall that for standard adaptive interpolation we have tolerances $tol_1^{in}, tol_2^{in}, tol_3^{in}$ (see subsection 4.1), whereas for directional variances-based adaptivity from subsection 4.2 we additionally have the directional tolerances $\{\tau_j^{in}\}_{j=1}^3$. We choose the FE mesh widths and adaptive interpolation tolerances such that the approximation errors are quantitatively similar. At level $\ell(1)$ we combine h_1 with tol_3^{in} and τ_3^{in} , at level $\ell(2)$, h_2 is combined with tol_2^{in} and τ_2^{in} , and at level $\ell(3)$ we employ h_3 together with tol_1^{in} and τ_1^{in} . For adaptive sparse grid quadrature we employ small tolerances $tol_1^{qu}, tol_2^{qu}, tol_3^{qu}$ to prevent the adaptive algorithm from stopping too early especially when integrating w.r.t. the prior density (recall Remark 5.1).

Since the source locations need to reside inside Ω , the prior is the uniform density in $[0, 1]^2$, i.e., $\pi_0 = U(0, 1)^2$. We consider 16 sensor locations at $(0.2i, 0.2j)$ for $i, j = 1, 2, 3, 4$. The measurements are obtained synthetically by discretizing the forward model on a finer mesh, i.e., $h = \sqrt{2}/2^7$ to avoid committing an “inverse crime.” Moreover, $\boldsymbol{\theta}_{\text{true}} = (0.35, 0.65)$ and the additive Gaussian noise $\boldsymbol{\eta} \sim N(\mathbf{0}, 0.2^2 I)$.

TABLE 3

Comparison of estimates of $\mathbb{E}[\pi^y(\theta)]$ for the source inversion problem with forward model (5.4). We first compute an MCMC solution using $2 \cdot 10^5$ MH samples. Afterward, we employ StdML and the two variants of our proposed multilevel approach, MLLejaStd and MLLejaDV.

Method	$\mathbb{E}_{\pi^y}[\theta]$
MH	(0.3628, 0.6370)
StdML	(0.3631, 0.6368)
MLLejaStd	(0.3630, 0.6369)
MLLejaDV	(0.3630, 0.6369)

The QoI is the posterior mean $\mathbb{E}_{\pi^y}[\theta]$. We compute a sampling solution using $2 \cdot 10^5$ samples obtained from a random walk MH algorithm with Gaussian proposal having covariance matrix $C_{\text{MH}} = 4 \cdot 10^{-3} I$, started from $\theta_0 = (1, 1)$. The acceptance rate of the chain is 64%. To obtain a comprehensive overview of the accuracy and cost of our approach, we compare it with the standard three-level approach in which all adaptive sparse grid operations are performed w.r.t. the prior density. Moreover, the QoI is assessed using the classical telescoping sum. To simplify the notation, in the following we use the abbreviation StdML to refer to the standard multilevel approach. MLLejaStd refers to our approach in which standard dimension-adaptive interpolation is used at each level, and MLLejaDV refers to our approach combined with directional variance-based adaptive interpolation summarized in subsection 4.2. The results are presented in Table 3. Observe that all multilevel methods yield results very close to the MCMC estimate. Thus, the two variants of our proposed approach, MLLejaStd and MLLejaDV, are comparably accurate as the sampling-based and the standard multilevel solutions.

In Figure 3, we visualize the results for all employed multilevel methods as follows. The left subplots show the results for StdML, whereas the center and right subplots depict the results for MLLejaStd and MLLejaDV, respectively. Furthermore, at each level, the prior as well as the corresponding (L)-Leja points used to find the interpolation surrogate are visualized in the top part. In the bottom plots, we depict the resulting posterior densities. At level $\ell(1)$ we obtain the same three posteriors since the prior is the same in all cases. However, starting with level $\ell(2)$ the sequential update of the auxiliary reference density in the proposed approach leads to significantly fewer interpolation points compared to StdML, which places a large number of weighted (L)-Leja points outside of the support of the corresponding posterior. Moreover, comparing the two variants of the proposed approach, MLLejaDV requires fewer (L)-Leja points than MLLejaStd. This is because at both levels $\ell(2)$ and $\ell(3)$ in MLLejaDV, the two total directional variances fall below the imposed tolerances. Thus MLLejaDV discovers and exploits more structure in the underlying approximation problem.

We visualize the multiindex sets for the three multilevel variants in Figure 4. At level $\ell(1)$ the multi-index sets corresponding to StdML and MLLejaStd are symmetric; this is because the two stochastic parameters have equal importance w.r.t. the prior density, which is the 2D (symmetric) uniform density. MLLejaDV leads to a smaller multi-index set since the directional variances τ_3^{in} fall below $(10^{-7}, 10^{-7})$, but there is no clear distinction between the two input directions as well. However, at level $\ell(2)$ we observe a different behavior in the two variants of our proposed approach, MLLejaStd and MLLejaDV. Recall that in these two variants the prior density is the Gaussian approximation of the posterior density from level $\ell(1)$. Computing the eigenvalues (λ_1, λ_2) of its covariance matrix, we obtain $\lambda_1 = 0.0097$ and $\lambda_2 = 0.0055$. Therefore, the first direction is more important than the second, which is reflected in

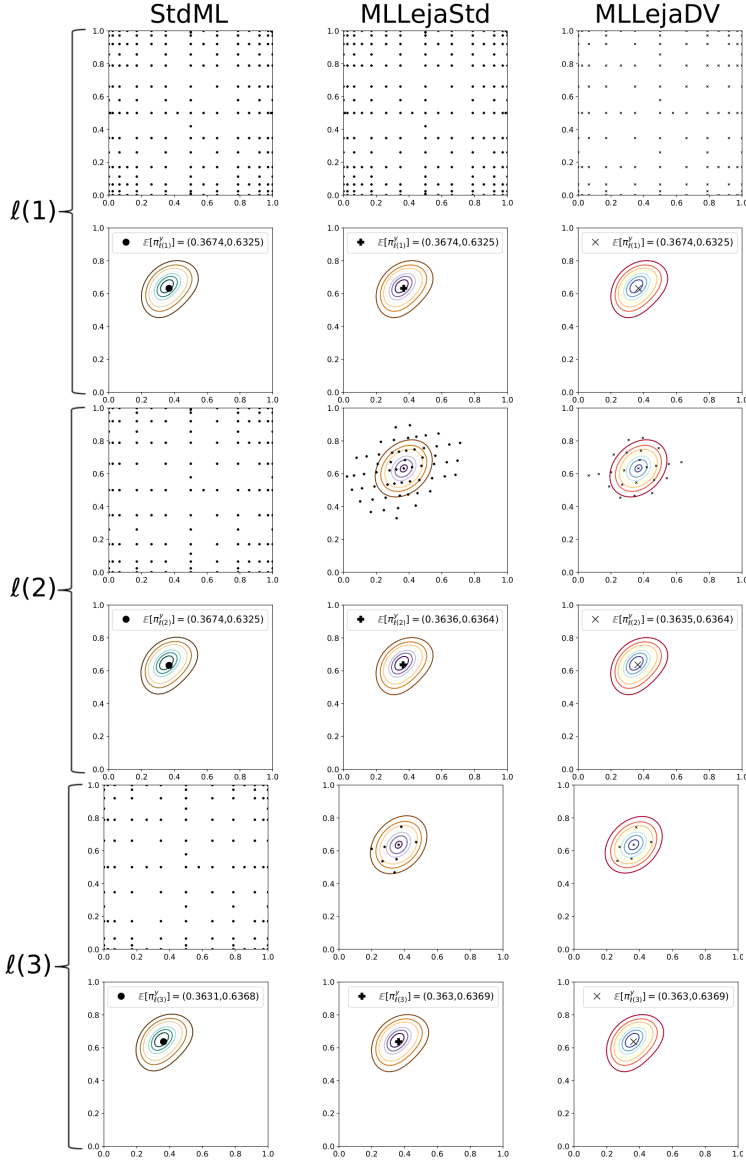


FIG. 3. Results obtained using StdML (left), MLLejaStd (center), and MLLejaDV (right) to find the adaptive sparse grid interpolation surrogate for the potential function in the source inversion problem with forward model (5.4). At each of the three levels, in the top plots we depict the prior density and the corresponding weighted (L)-Leja points used to find the surrogate. At levels $\ell(2)$ and $\ell(3)$, the prior is the Gaussian approximation of the posterior from the posterior level. In the bottom plots we depict the corresponding posterior density solution.

the two multi-index sets. On the other hand, the multi-index set for the standard approach remains symmetric because the prior density is unchanged. Finally, at level $\ell(3)$ we see low-cardinality multi-index sets for both MLLejaStd and MLLejaDV. This is because at this stage we have an informative prior, thus the likelihood ratio is close to 1, which requires little approximation effort. Hence going beyond level $\ell(3)$ is not necessary for our approach.

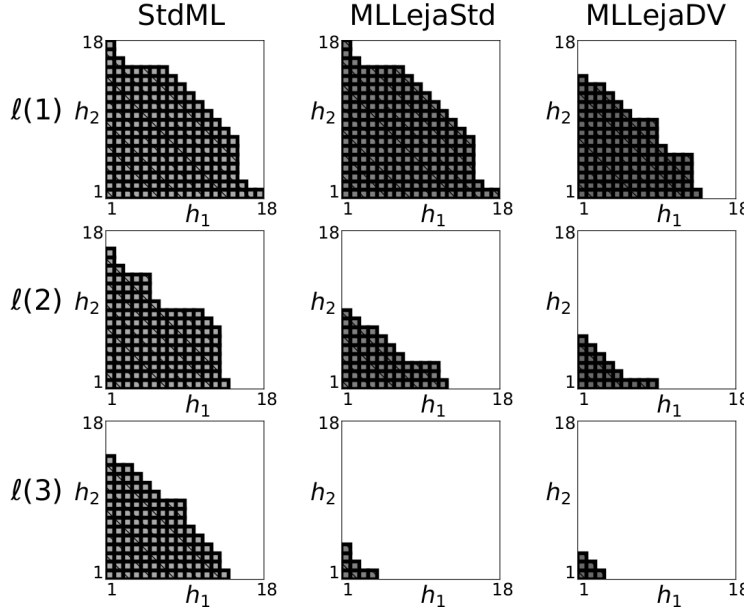


FIG. 4. Multi-index sets corresponding to adaptive sparse grid interpolation in the source inversion problem (5.4) for StdML (left), MLLejaStd (center), and MLLejaDV (right).

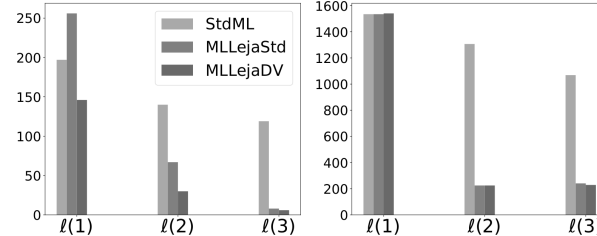


FIG. 5. Left: Total number of forward model evaluations needed in the adaptive sparse interpolation of the potential using the three multilevel variants in the source inversion problem (5.4). Right: Total number of quadrature nodes.

The costs of all multilevel methods are visualized in Figure 5. The number of forward model evaluations needed to find the adaptive sparse grid surrogate of the potential function are shown on the left side. In the right plot we depict the number of evaluations of the surrogate in all quadrature computations. Note in all multilevel variants we need quadrature to assess the evidences and expectations at all three levels. Additionally, in MLLejaStd and MLLejaDV we need to compute the covariance matrices at levels $\ell(1)$ and $\ell(2)$ as well, which are needed in the Gaussian approximation of the associated posteriors and affine mapping (recall (3.1) and (3.2)). However, since we integrate w.r.t. the same weight function, we keep all surrogate evaluations in a look-up table and reuse them whenever the same grid points are used for different evaluations. We observe that at level $\ell(1)$ our proposed approach is slightly more expensive for interpolation, which is due to the need to evaluate the FE solver on level $\ell(1)$ at level $\ell(2)$ as well: recall that at level $\ell(2)$ we construct a sparse grid surrogate for the ratio of potential functions. However, the increased cost is not significant since

it involves evaluations of the coarsest FE solver, which are very fast. Starting with level $\ell(2)$ we see significant cost savings for both interpolation and quadrature. On the one hand, at level $\ell(2)$, MLLejaStd leads to about 2 times fewer forward model evaluations for sparse grid interpolation and around 12.5 fewer sparse grid quadrature evaluations. Moreover, at level $\ell(3)$ we obtain about 15 times fewer interpolation points and 7.5 times fewer quadrature nodes. On the other hand, MLLejaDV leads to about 5 times fewer interpolation nodes and about 12.5 times fewer quadrature evaluations. Furthermore, we obtain 20 times fewer interpolation nodes and 9.5 times fewer quadrature nodes at level $\ell(3)$. These results clearly show that updating the prior information in our multilevel approach for Bayesian inversion leads to significant cost reduction in finding and evaluating sparse grid surrogates.

5.3. Source inversion with two sources in a 2D spatial domain. For a more comprehensive overview of the proposed approach, we consider now a test case with multimodal observation data. In particular, we consider another source inversion test case in which we use two sources to generate the data—to have bimodal observation data—and only one source to perform the Bayesian inference.

The elliptic forward operator defined on $\Omega := [0, 1]^2$ reads

$$(5.5) \quad \begin{aligned} -(u_{xx} + u_{yy})(x, y) &= A(\alpha) \left(\exp(-[(x - \theta_1)^2 + (y - \theta_2)^2]/2\alpha^2) \right. \\ &\quad \left. + b \exp(-[(x - \theta_3)^2 + (y - \theta_4)^2]/2\alpha^2) \right), \quad (x, y) \in \Omega, \\ u(x, y) &= 0, \quad (x, y) \in \partial\Omega, \end{aligned}$$

where $A(\alpha) = 5/(2\pi\alpha^2)$, $\alpha = 0.15$, and the binary parameter $b = 1$ when generating the data and $b = 0$ when performing the inference. Therefore, we are solving a source inversion similar to the one in subsection 5.2 but starting from bimodal data.

To generate the data we choose the locations of the two sources far apart, i.e., $(\theta_1, \theta_2)_{\text{true}} = (0.15, 0.15)$ and $(\theta_3, \theta_4)_{\text{true}} = (0.85, 0.85)$. For Bayesian inference we employ StdML, MLLejaStd, and MLLejaDV using three levels. The multilevel setup is outlined in Table 4.

We visualize in Figure 6 the bimodal posterior density obtained via standard Bayes' formula (2.3) for which we used $50^2 = 2500$ Gauss-Legendre points to assess the evidence. Note that the two peaks are symmetric around $(0.5, 0.5)$. Therefore, Bayesian inference using only once source in the forward model can yield, in the best case, a posterior density centered at $(0.5, 0.5)$.

The QoI is again $\mathbb{E}[\pi^y(\boldsymbol{\theta})]$. In Table 5 we show the obtained estimates. First, an MH estimate with $2 \cdot 10^5$ samples is computed using a random walk Gaussian proposal with initial sample $\boldsymbol{\theta}_0 = (1.0, 1.0)$ and covariance matrix $C_{\text{MH}} = 10^{-1}I$. The acceptance rate is 45%. We observe that the MH and StdML solutions yield estimates close to the center, $(0.5, 0.5)$. However, the estimates given by MLLejaStd and MLLejaDV are far away from this value.

TABLE 4
Multilevel setup for the 2D inversion problem with forward model (5.5).

Level	h	tol^{in}	τ^{in}	tol^{qu}
$\ell(1)$	$h_1 = \sqrt{2}/2^5$	$tol_3^{\text{in}} = 10^{-6}$	$\tau_3^{\text{in}} = (10^{-8}, 10^{-8})$	$tol_3^{\text{qu}} = 10^{-13}$
$\ell(2)$	$h_2 = \sqrt{2}/2^6$	$tol_2^{\text{in}} = 10^{-5}$	$\tau_2^{\text{in}} = (10^{-7}, 10^{-7})$	$tol_2^{\text{qu}} = 10^{-12}$
$\ell(3)$	$h_3 = \sqrt{2}/2^7$	$tol_1^{\text{in}} = 10^{-4}$	$\tau_1^{\text{in}} = (10^{-6}, 10^{-6})$	$tol_1^{\text{qu}} = 10^{-11}$

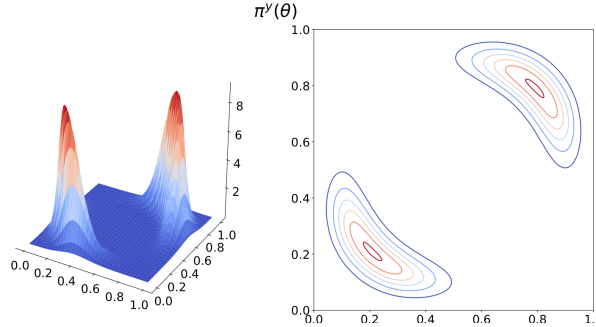


FIG. 6. Posterior density for the source inversion problem with forward model (5.5). We used $50^2 = 2500$ Gauss-Legendre points to assess the evidence.

TABLE 5

Comparison of estimates of $\mathbb{E}[\pi^y(\theta)]$ for the source inversion problem with forward model (5.5). We first compute a sampling solution using $2 \cdot 10^5$ MH samples. Afterward, we employ StdML and the two variants of our proposed multilevel approach, MLLejaStd and MLLejaDV.

Method	$\mathbb{E}_{\pi^y}[\theta]$
MH	(0.5032, 0.5068)
StdML	(0.5002, 0.5002)
MLLejaStd	(0.6688, 0.6548)
MLLejaDV	(0.6648, 0.6548)

We depict in Figure 7 the prior and posterior density as well as the weighted (L)-Leja points used to construct the adaptive sparse grid interpolation surrogate of the potential function for all employed multilevel methods. We observe that the Gaussian approximation used in our proposed approach at levels $\ell(2)$ and $\ell(3)$ is very spread and quite different from the approximated posterior. Hence the bias-correcting ratio in quadrature operations, $\pi_{\ell(j)}^y / \hat{\pi}_{\ell(j)}^y$ for $j = 2, 3$ (recall (3.3)) is different from 1 in most regions of the domain. The large variations of this ratio lead to large variations of the error indicators in adaptive sparse grid quadrature which prevent the algorithm from converging and hence yield accurate estimates. Therefore, the estimates of the expectation and covariance matrix of the posteriors from levels $\ell(1)$ and $\ell(2)$, and with that, the Gaussian approximations employed at levels $\ell(2)$ and $\ell(3)$, are inaccurate. Note that the large spread of the Gaussian approximations leads to weighted (L)-Leja points outside of the domain of the uniform prior, which coincides with the domain of the forward operator, Ω (see (5.5)). Whenever this happens, we impose the corresponding likelihood evaluation to be zero.

5.4. Higher-dimensional problem in a 3D spatial domain. In the final test case, we apply the proposed approach in a more challenging and computationally more expensive problem. We consider an elliptic forward model defined on $\Omega := [0, 1]^3$ with a permeability field projected onto a Fourier basis:

$$(5.6) \quad \begin{aligned} -\nabla \cdot (k(x, y, z, \theta) \nabla u(x, y, z)) &= f, & (x, y, z) \in \Omega, \\ u(x, y, z) &= 0, & (x, y, z) \in \partial\Omega, \end{aligned}$$

where $f \equiv 5$ and

$$(5.7) \quad k(x, y, z, \theta) := \exp \left(\sum_{n=1}^8 s_n \theta_n \sin(p_{n,1}\pi x) \sin(p_{n,2}\pi y) \sin(p_{n,3}\pi z) \right),$$

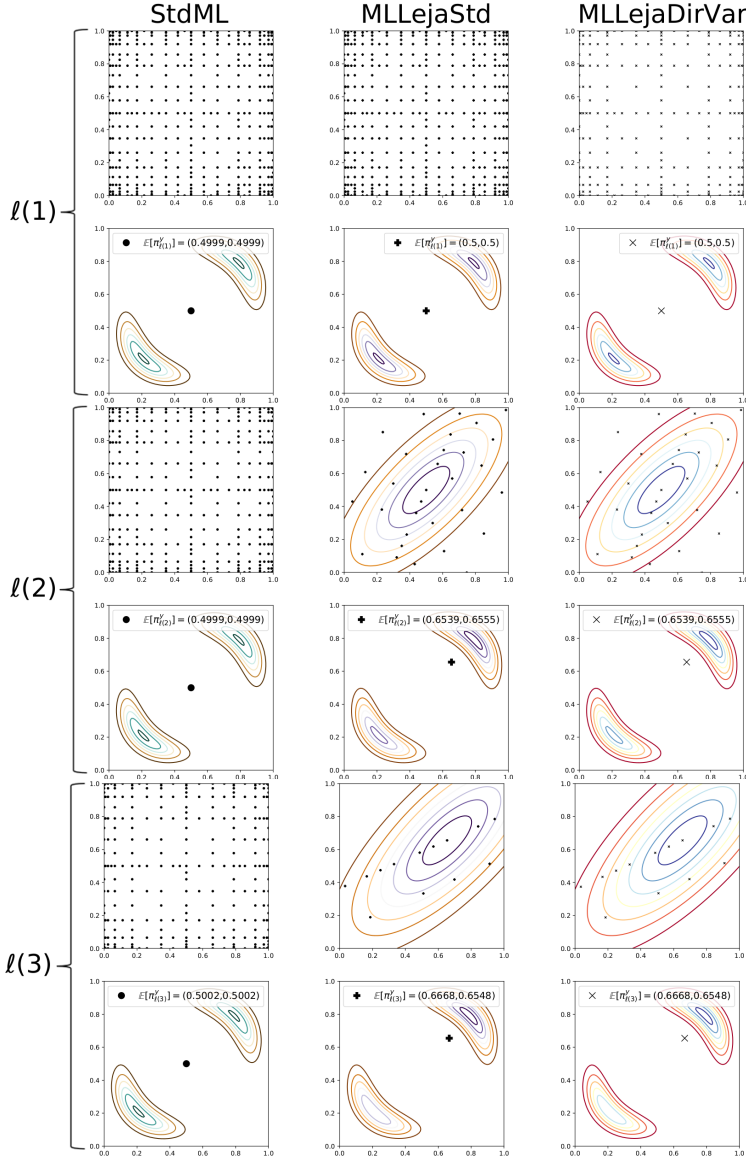


FIG. 7. Results obtained using StdML (left), MLLejaStd (center), and MLLejaDV (right) to find the adaptive sparse grid interpolation surrogate for the potential function in the source inversion problem with forward model (5.5). At each of the three levels, in the top plots we depict the prior density and the corresponding weighted (L)-Leja points used to find the surrogate. At levels $\ell(2)$ and $\ell(3)$, the prior is the Gaussian approximation of the posterior from the posterior level. In the bottom plots we depict the corresponding posterior density solution.

where $s_1 = 0.1785$, $s_2 = s_3 = s_4 = 0.1428$, $s_5 = s_6 = s_7 = 0.1071$, $s_8 = 0.0714$ are normalized scaling factors, i.e., $\sum_{n=1}^8 s_n = 1$, and $(p_{n,1}, p_{n,2}, p_{n,3}) \in \{1, 2\}^3$. Note that with the chosen setup, θ_1 is the most important parameter, $\theta_2, \theta_3, \theta_4$ are the second most important parameters, etc., under the prior density.

Bayesian inference is carried out for the weights $(\theta_1, \theta_2, \dots, \theta_8)$ of the permeability field $k(x, y, z, \boldsymbol{\theta})$. Thus, we are solving an 8D inversion problem. These weights follow

TABLE 6
Multilevel setup for the 8D inversion problem with forward model (5.6).

Level	h	tol^{in}	τ^{in}	tol^{qu}
$\ell(1)$	$h_1 = \sqrt{3}/2^4$	$tol_3^{in} = 10^{-5}$	$\tau_3^{in} = 10^{-7} \cdot \mathbf{1}_8$	$tol_3^{qu} = 10^{-9}$
$\ell(2)$	$h_2 = \sqrt{3}/2^5$	$tol_2^{in} = 10^{-4}$	$\tau_2^{in} = 10^{-6} \cdot \mathbf{1}_8$	$tol_2^{qu} = 10^{-8}$
$\ell(3)$	$h_3 = \sqrt{3}/2^6$	$tol_1^{in} = 10^{-3}$	$\tau_1^{in} = 10^{-5} \cdot \mathbf{1}_8$	$tol_1^{qu} = 10^{-7}$

a standard normal prior distribution, i.e., $\mu_0 = N(\mathbf{0}, I)$. To perform the Bayesian inference we employ both the standard and our proposed multilevel approach with the two variants, MLLejaStd and MLLejaDV, considering $J = 3$. The employed multilevel setup is outlined in Table 6. The forward model (5.6) is discretized via standard tetrahedral FE meshes h_j . Moreover, the sparse grid interpolation tolerances tol_j^{in} and τ_j^{in} are chosen to yield quantitatively similar errors to the FE approximation for $j = 1, 2, 3$. Finally, we choose small tolerances for quadrature to prevent the adaptive algorithm from stopping too early.

The observation data consists of 729 measurements at $\{0.1, 0.2, \dots, 0.9\}^3 \in \Omega$, stemming from the FE solution of the forward model discretized using a finer mesh width $h = \sqrt{3}/2^7$ and assuming measurement noise $\eta \sim N(\mathbf{0}, 0.1^2 I)$. In addition, θ_{true} is drawn from the standard multivariate Gaussian density, i.e.,

$$\theta_{true} = (0.3015, 0.6578, -0.5002, 0.4608, 1.1345, 0.5447, -1.5353, -0.1689).$$

The QoI is again the expectation of the posterior density, $E_{\pi^y}[\theta]$. We begin with level $\ell(1)$ in the standard multilevel approach. Both the expectation and the covariance matrix of the corresponding posterior are computed since we need these evaluations at $\ell(2)$. We obtain, however, an indefinite covariance matrix with a negative variance for θ_1 . This is mainly due to the limitations of the standard approach: adaptive sparse grid quadrature w.r.t. the prior density becomes challenging when the complexity of the underlying Bayesian inverse problem increases. To overcome this limitation, we employ instead a standard (L)-Leja sparse grid of an a priori fixed level having sufficiently many points to guarantee a positive definite covariance matrix. In particular, we consider an interpolation grid of level 10 for interpolation (24310 grid points) and a quadrature grid of the same level comprising 598417 points. Since our goal is to compare multilevel methods based on adaptive sparse grid algorithms, we do not perform the standard multilevel approach on the remaining two levels using a priori chosen sparse grids, but rather focus only on the two variants of our proposed approach starting from the Gaussian approximation of the posterior at level $\ell(1)$ obtained with the aforementioned standard sparse grids. Moreover, evaluating the FE discretizations depending on h_2 and h_3 on the standard sparse grid of level 10 (24310 evaluations) requires a significant computational cost.

We first compute an MH solution with 10^5 samples. The Gaussian proposal has covariance matrix $C_{MH} = 0.5I$. To reduce the burn-in, the chain is started from θ_{true} . The acceptance rate is 24%. Afterward, we employ MLLejaStd and MLLejaDV as described above. The results are showed in Table 7. The two variants of our approach produce results comparable to the sampling solution, thus making our proposed approach competitive with sampling methods in this test case as well. Observe, however, that the accuracy of all estimates deteriorates compared with θ_{true} . This is because the likelihood becomes less informative as the index increases from 1 to 8: the likelihood updates the prior very well for the first direction, relatively well

TABLE 7

Estimation of the posterior's mean value for the fourth test case using a reference MH solution with 10^5 samples and the two variants of our proposed multilevel approach for Bayesian inversion.

Method	$\mathbb{E}_{\pi^y}[\theta_1]$	$\mathbb{E}_{\pi^y}[\theta_2]$	$\mathbb{E}_{\pi^y}[\theta_3]$	$\mathbb{E}_{\pi^y}[\theta_4]$	$\mathbb{E}_{\pi^y}[\theta_5]$	$\mathbb{E}_{\pi^y}[\theta_6]$	$\mathbb{E}_{\pi^y}[\theta_7]$	$\mathbb{E}_{\pi^y}[\theta_8]$
MH	0.2532	0.2123	-0.1363	0.1326	0.1486	0.0753	-0.1584	0.0066
MLStd	0.2642	0.2111	-0.1630	0.1539	0.1429	0.0670	-0.1816	-0.0053
MLDV	0.2620	0.2114	-0.1600	0.1542	0.1448	0.0689	-0.1808	-0.0050

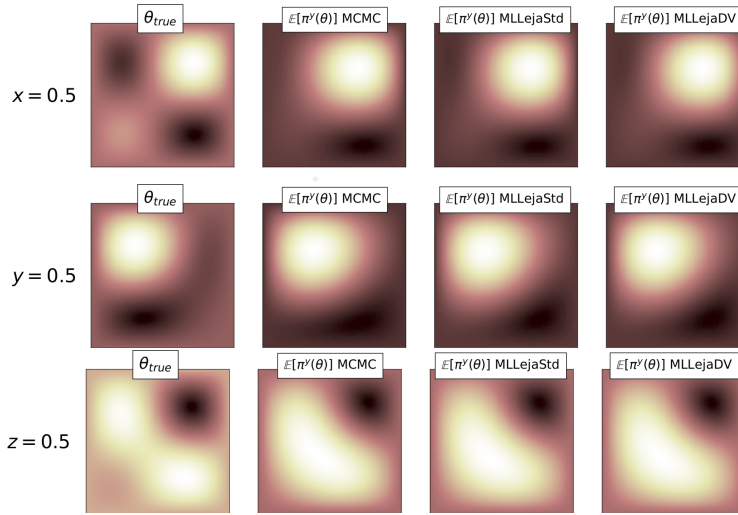


FIG. 8. 2D slices of the 3D permeability field from (5.7) parametrized using θ_{true} and the mean estimates from Table 7. Top: yz slice taking $x = 0.5$. Middle: xz slice when $y = 0.5$. Bottom: xy slice fixing $z = 0.5$.

for the next three, and almost not at all for the last four directions. Nevertheless, since the last four directions are the least important by construction (5.7) we expect that not having accurate corresponding mean estimates will not be too significant.

To assess the quality of the expectation estimates, we use them to represent the permeability field as $k(x, y, z, \mathbb{E}_{\pi^y}[\theta])$ and we compare the results with $k(x, y, z, \theta_{true})$. In Figure 8 we depict 2D slices of the field in which the spatial coordinates x (top), y (middle), and z (bottom) are fixed respectively to 0.5. We observe that having inaccurate estimates for the latter four components of θ does not significantly affect the estimation of the true permeability field. This is due to having good estimates for the first components of θ_{true} , which are the most important by construction.

In Figure 9 the costs for interpolation (left) and quadrature (right) are shown. Note that for interpolation we show costs for level $\ell(1)$ as well because evaluations of the forward PDE discretized using h_1 are needed at $\ell(2)$. MLLejaDV is cheaper than MLLejaStd at all three levels, requiring about 4.3 times fewer evaluations at level $\ell(1)$, 4.8 times fewer evaluations on level $\ell(2)$, and 7 times fewer evaluations at level $\ell(3)$. Observe that the overall interpolation costs are very small given that we have an 8D inversion problem at hand. For example, at level $\ell(3)$, MLLejaDV requires only 22 PDE evaluations. The maximum reached level in the corresponding multi-index set is 4 and all its multi-indices have components larger than 1 only in the first four directions. Indeed, the directional variances-based algorithm detects that the latter four directions are unimportant and thus invests effort only in the first four directions.

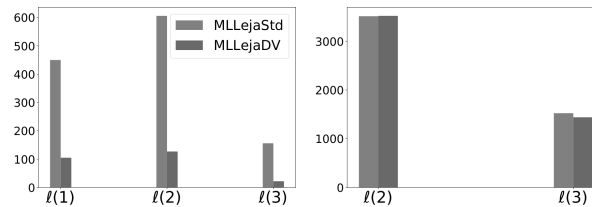


FIG. 9. Left: Total number of forward model evaluations needed by the two variants of our proposed approach, MLLejaStd and MLLejaDV, at all three levels in the 8D inversion problem with forward model (5.6). Right: Total number of quadrature nodes used in all three in MLLejaStd and MLLejaDV at levels $\ell(2)$ and $\ell(3)$.

Therefore, we see once again that using the enhanced adaptive algorithm for adaptive sparse grid interpolation leads to significant cost savings. For quadrature, the total number of evaluations of the interpolation surrogates are similar.

6. Conclusions. We proposed a novel multilevel Leja algorithm for computing posterior approximations in computationally expensive, higher-dimensional Bayesian inverse problems. At each level adaptive sparse grid interpolation is employed to find a surrogate of the potential function, and adaptive sparse grid quadrature is then used to perform all integration operations with respect to the posterior. We considered two adaptive strategies for interpolation: (i) a standard method and (ii) an enhanced adaptive algorithm in which directional variances are used to ensure that only the most important stochastic directions are refined. The backbone of the proposed approach is the sequential update of the auxiliary reference density. In this way, we can create weighted (L)-Leja points in areas of high posterior probability. Numerical experiments with elliptic inverse problems in 2D and 3D space show that the sequential update of the auxiliary density leads to considerably fewer model evaluations compared to the standard multilevel approach which employs the prior density at all levels. We remark that the proposed approach is not designed to handle well multimodal posterior densities. In future research we will extend it such that it employs more general nonlinear mappings, e.g., transport maps, to accurately approximate arbitrary, multimodal posteriors.

Acknowledgment. We want to thank the anonymous reviewers for their insightful suggestions and comments.

REFERENCES

- [1] S. BROOKS, A. GELMAN, G. L. JONES, AND X.-L. MENG, *Handbook of Markov Chain Monte Carlo*, Chapman & Hall/CRC Handb. Mod. Stat. Methods, CRC Press, Boca Raton, FL, 2011.
- [2] H.-J. BUNGARTZ AND M. GRIEBEL, *Sparse grids*, Acta Numer., 13 (2004), pp. 147–269.
- [3] P. CHEN AND C. SCHWAB, *Sparse-grid, reduced-basis Bayesian inversion*, Comput. Methods Appl. Mech. Engrg., 297 (2015), pp. 84–115.
- [4] P. CHEN AND C. SCHWAB, *Adaptive sparse grid model order reduction for fast Bayesian estimation and inversion*, in Sparse Grids and Applications—Stuttgart 2014, Lect. Notes Comput. Sci. Eng. 109, Springer, Cham, 2016, pp. 1–27.
- [5] P. CHEN, U. VILLA, AND O. GHATTAS, *Hessian-based adaptive sparse quadrature for infinite-dimensional Bayesian inverse problems*, Comput. Methods Appl. Mech. Engrg., 327 (2017), pp. 147–172.
- [6] P. CONRAD AND Y. MARZOUK, *Adaptive Smolyak pseudospectral approximations*, SIAM J. Sci. Comput., 35 (2013), pp. A2643–A2670.

- [7] P. DEL MORAL, A. DOUCET, AND A. JASRA, *Sequential Monte Carlo samplers*, J. R. Stat. Soc. Ser. B Stat. Methodol., 68 (2006).
- [8] J. DICK, R. N. GANTNER, Q. T. LE GIA, AND C. SCHWAB, *Multilevel higher-order quasi-Monte Carlo Bayesian estimation*, Math. Models Methods Appl. Sci., 27 (2017), pp. 953–995.
- [9] T. DODWELL, C. KETELSEN, R. SCHEICHL, AND A. TECKENTRUP, *A hierarchical multilevel Markov chain Monte Carlo algorithm with applications to uncertainty quantification in subsurface flow*, SIAM/ASA J. Uncertain. Quantif., 3 (2015), pp. 1075–1108.
- [10] S. E. DOSSO, C. W. HOLLAND, AND M. SAMBRIDGE, *Parallel tempering for strongly nonlinear geoacoustic inversion*, J. Acoust. Soc. Am., 132 (2012), pp. 3030–3040.
- [11] M. EIGEL, M. MARSCHALL, AND R. SCHNEIDER, *Sampling-free Bayesian inversion with adaptive hierarchical tensor representations*, Inverse Problems, 34 (2018), 035010.
- [12] O. G. ERNST, B. SPRUNGK, AND L. TAMELLINI, *On Expansions and Nodes for Sparse Grid Collocation of Lognormal Elliptic PDEs*, <https://arxiv.org/abs/1906.01252>, 2019.
- [13] I.-G. FARCAŞ, T. GÖRLER, H.-J. BUNGARTZ, F. JENKO, AND T. NECKEL, *Sensitivity-Driven Adaptive Sparse Stochastic Approximations in Plasma Microinstability Analysis*, <https://arxiv.org/abs/1812.00080>, 2018.
- [14] I.-G. FARCAŞ, P. C. SÂRBU, H.-J. BUNGARTZ, T. NECKEL, AND B. UEKERMANN, *Multi-level adaptive stochastic collocation with dimensionality reduction*, in *Sparse Grids and Applications—Miami 2016*, J. Garcke, D. Pflüger, C. G. Webster, and G. Zhang, eds., Springer, Cham, 2018, pp. 43–68.
- [15] M. FRANGOS, Y. MARZOUK, K. WILLCOX, AND B. VAN BLOEMEN WAANDERS, *Surrogate and reduced-order modeling: A comparison of approaches for large-scale statistical inverse problems*, in *Large-Scale Inverse Problems and Quantification of Uncertainty*, Wiley Ser. Comput. Stat., Wiley, Chichester, UK, 2011, pp. 123–149.
- [16] N. GEORG, D. LOUKREZIS, U. RÖMER, AND S. SCHÖPS, *Uncertainty Quantification for an Optical Grating Coupler with an Adjoint-Based Leja Adaptive Collocation Method*, CoRR, <https://arxiv.org/abs/1807.07485>, 2018.
- [17] T. GERSTNER AND M. GRIEBEL, *Dimension-adaptive tensor-product quadrature*, Computing, 71 (2003), pp. 65–87.
- [18] M. GRIEBEL, M. SCHNEIDER, AND C. ZENGER, *A combination technique for the solution of sparse grid problems*, in *Iterative Methods in Linear Algebra*, P. de Groen and R. Beauwens, eds., North-Holland, Amsterdam, 1992, pp. 263–281.
- [19] J. HADAMARD, *Sur les problèmes aux dérivées partielles et leur signification physique*, Princeton Univ. Bull., 13 (1902), pp. 49–52.
- [20] M. HEGLAND, *Adaptive sparse grids*, Anziam J., 44 (2003), pp. C335–C353.
- [21] K. ITO AND B. JIN, *Inverse Problems: Tikhonov Theory and Algorithms*, World Scientific, Singapore, 2014.
- [22] P. JANTSCH, C. G. WEBSTER, AND G. ZHANG, *On the Lebesgue constant of weighted Leja points for Lagrange interpolation on unbounded domains*, IMA J. Numer. Anal., 39 (2018), pp. 1039–1057.
- [23] L. JIANG AND N. OU, *Bayesian inference using intermediate distribution based on coarse multiscale model for time fractional diffusion equations*, Multiscale Model. Simul., 16 (2018), pp. 327–355.
- [24] J. KAPIO AND E. SOMERSALO, *Statistical and Computational Inverse Problems*, Appl. Math. Sci., 160, Springer-Verlag, New York, 2005.
- [25] M. C. KENNEDY AND A. O'HAGAN, *Bayesian calibration of computer models*, J. R. Stat. Soc. Ser. B Stat. Methodol., 63 (2001), pp. 425–464.
- [26] J. LATZ, *On the Well-posedness of Bayesian Inverse Problems*, <https://arxiv.org/abs/1902.10257>, 2019.
- [27] J. LATZ, M. EISENBERGER, AND E. ULLMANN, *Fast sampling of parameterised Gaussian random fields*, Comput. Methods Appl. Mech. Eng., 348 (2019), pp. 978–1012.
- [28] J. LATZ, I. PAPAIOANNOU, AND E. ULLMANN, *Multilevel sequential² Monte Carlo for Bayesian inverse problems*, J. Comput. Phys., 368 (2018), pp. 154–178.
- [29] J. LI AND Y. M. MARZOUK, *Adaptive construction of surrogates for the Bayesian solution of inverse problems*, SIAM J. Sci. Comput., 36 (2014), pp. A1163–A1186.
- [30] C. LIEBERMAN, K. WILLCOX, AND O. GHATTAS, *Parameter and state model reduction for large-scale statistical inverse problems*, SIAM J. Sci. Comput., 32 (2010), pp. 2523–2542.
- [31] X. MA AND N. ZABARAS, *An efficient Bayesian inference approach to inverse problems based on an adaptive sparse grid collocation method*, Inverse Problems, 25 (2009), 035013.
- [32] Y. MARZOUK, T. MOSELHY, M. PARNO, AND A. SPANTINI, *Sampling via measure transport: An introduction*, in *Handbook of Uncertainty Quantification*, Springer, Cham, 2016, pp. 1–41.

- [33] Y. MARZOUK AND D. XIU, *A stochastic collocation approach to Bayesian inference in inverse problems*, Commun. Comput. Phys., 6 (2009), pp. 826–847.
- [34] S. A. MATTIS AND B. WOHLMUTH, *Goal-oriented adaptive surrogate construction for stochastic inversion*, Comput. Methods Appl. Mech. Engrg., 339 (2018), pp. 36–60.
- [35] A. NARAYAN AND J. D. JAKEMAN, *Adaptive Leja sparse grid constructions for stochastic collocation and high-dimensional approximation*, SIAM J. Sci. Comput., 36 (2014), pp. A2952–A2983.
- [36] B. PEHERSTORFER AND Y. MARZOUK, *A Transport-Based Multifidelity Preconditioner for Markov Chain Monte Carlo*, <https://arxiv.org/abs/1808.09379>, 2018.
- [37] B. PEHERSTORFER, K. WILLCOX, AND M. GUNZBURGER, *Survey of multifidelity methods in uncertainty propagation, inference, and optimization*, SIAM Rev., 60 (2018), pp. 550–591.
- [38] R. SCHEICHL, A. STUART, AND A. TECKENTRUP, *Quasi-Monte Carlo and multilevel Monte Carlo methods for computing posterior expectations in elliptic inverse problems*, SIAM/ASA J. Uncertain. Quantif., 5 (2017), pp. 493–518.
- [39] C. SCHILLINGS AND C. SCHWAB, *Sparse, adaptive Smolyak quadratures for Bayesian inverse problems*, Inverse Problems, 29 (2013), 065011.
- [40] C. SCHILLINGS AND C. SCHWAB, *Sparsity in Bayesian inversion of parametric operator equations*, Inverse Problems, 30 (2014), 065007.
- [41] C. SCHWAB AND A. M. STUART, *Sparse deterministic approximation of Bayesian inverse problems*, Inverse Problems, 28 (2012), 045003.
- [42] S. SMOLYAK, *Quadrature and interpolation formulas for tensor products of certain classes of functions*, Soviet Math. Dokl., 4 (1963), pp. 240–243.
- [43] I. M. SOBOL', *Global sensitivity indices for nonlinear mathematical models and their monte carlo estimates*, Math. Comput. Simul., 55 (2001), pp. 271–280.
- [44] A. STUART, *Inverse problems: A Bayesian perspective*, Acta Numer., 19 (2010), pp. 451–559.
- [45] A. STUART AND A. TECKENTRUP, *Posterior consistency for Gaussian process approximations of Bayesian posterior distributions*, Math. Comp., 87 (2018), pp. 721–753.
- [46] B. SUDRET, *Global sensitivity analysis using polynomial chaos expansions*, Reliab. Eng. Syst. Safe., 93 (2008), pp. 964–979.
- [47] A. TARANTOLA, *Inverse Problem Theory and Methods for Model Parameter Estimation*, SIAM, Philadelphia, 2005.
- [48] R. TEMPONE AND S. WOLFERS, *Smolyak's algorithm: A powerful black box for the acceleration of scientific computations*, in Sparse Grids and Applications—Miami 2016, J. Garcke, D. Pflüger, C. G. Webster, and G. Zhang, eds., Springer, Cham, 2018, pp. 201–228.
- [49] J. WINOKUR, D. KIM, F. BISETTI, O. P. LE MAÎTRE, AND O. M. KNIO, *Sparse pseudo spectral projection methods with directional adaptation for uncertainty quantification*, J. Sci. Comput., 68 (2016), pp. 596–623.
- [50] L. YAN AND Y.-X. ZHANG, *Convergence analysis of surrogate-based methods for Bayesian inverse problems*, Inverse Problems, 33 (2017), 125001.
- [51] L. YAN AND T. ZHOU, *Adaptive multi-fidelity polynomial chaos approach to Bayesian inference in inverse problems*, J. Comput. Phys., 381 (2019), pp. 110–128.